Fe e-Front runners

FUJI ELECTRIC
REVIEW

2

2008 VOL.54

Semiconductors

Fuji Electric Group

FUJI ELECTRIC REVIEW

2
2008 VOL.54

Semiconductors

CONTENTS

Cover photo:

The automotive industry's environmental activities are increasing at the same time as environmental regulations in various countries throughout the world are being strengthened. To comply with such regulations, the systems used in automobiles are becoming more efficient and are achieving higher control accuracy day-by-day. Moreover, engine management for measuring pressure and implementing control has become increasingly important in these systems. Fuji Electric, which began mass-producing automotive pressure sensors in 1984, has proposed proprietary high reliability circuit technology and advanced MEMS (micro electro mechanical systems) technology in response to strict cost requirements and changing needs for accuracy, and Fuji Electric's automotive pressure sensors are being used in automobiles and motorcycles both in Japan and overseas.

The cover photo shows an example of a 5th generation digital trimming type automotive miniature pressure sensor chip and package. This chip is implemented in a more compact size while maintaining the same functions, performance and EMC (electromagnetic compatibility) protection performance as the 4th generation chip which is already in mass-production.

Fuji Electric's Semiconductors: Present Status and Future Outlook

Tatsuhiko Fujihira
**Hisao Shigekane**

1. Introduction

In the chairman's summary statement of the G8 Summit held in Heiligendamm, Germany in early June 2007, it was announced that the G8 nations would "devote serious effort to decrease global greenhouse gas emissions at least by half by 2050." Behind this statement is the IPCC's (Intergovernmental Panel on Climate Change) 4th Assessment Report[1]. This report concluded that the cause of global weather changes over the past 50 years in the latter half of the 20th century, as typified by the average temperature rise and average sea level rise, is attributable with greater than 90% certainty to an increased concentration of greenhouse gas due to human activities. In comparison to the 3rd Assessment Report which reached the same conclusion but with a certainty of slightly greater than 66%, it can be concluded that mankind is obligated to make drastic reductions in greenhouse gas emissions, chiefly CO_2. For reference, Fig. 1 is an excerpt from the 4th Assessment Report and shows the changes in CO_2 concentration in the atmosphere over the past 10,000 years. The sudden increase in CO_2 concentration over the past 50 years is likely to be judged abnormal by anyone who views this chart. It can be understood in-

Fig.1 Changes in the global atmospheric concentration of carbon dioxide over the past 10,000 years[2]

tuitively that a significant reduction in greenhouse gas emissions must be pursued urgently.

Promoting "harmony with nature" as a basic philosophy, the entire Fuji Electric Group is committed to protecting the global environment by providing products and technologies that contribute to the protection of the global environment, reducing the burden on the environment during product lifecycles and reducing the burden of business activities on the environment as pillars of basic policy for environment protection. Fuji Electric Group is concentrating on power electronics, which aims to utilize electric power energy effectively, and power semiconductors, which are the key components of power electronics, as an important business that will contribute to global environmental protection and especially to a reduction in CO_2 emissions. Electrical power generation accounts for approximately 40% of primary energy consumption, and because that percentage is predicted[2] to increase steadily, the importance of power electronics and power semiconductors is expected to increase in the future.

The role of power semiconductor in reducing CO_2 emissions is to increase the utilization efficiency of power electronics equipment, and to be effective in conserving resources (through miniaturization) and expanding utilization (through lower cost and an expanded range of applications). More specifically, the trends toward lower loss and lower noise, smaller size, higher reliability, lower cost, and expansion of the product series and applications must be advanced. In order to achieve lower loss, switching loss must be reduced, but recklessly increasing the switching speed causes the generated electromagnetic noise to increase, resulting in incorrect operation of the control system and peripheral equipment. Accordingly, a tradeoff relation exists between lower loss and lower noise, and both low loss and low noise are being requested of recent power semiconductors. Lower loss contributes to improved power utilization efficiency, and lower noise contributes to a reduction in the number of anti-noise components and resource conservation. Miniaturization, higher reliability and lower cost contribute to resource conservation in power semiconductors themselves and in power electronics equipment, and longer service life
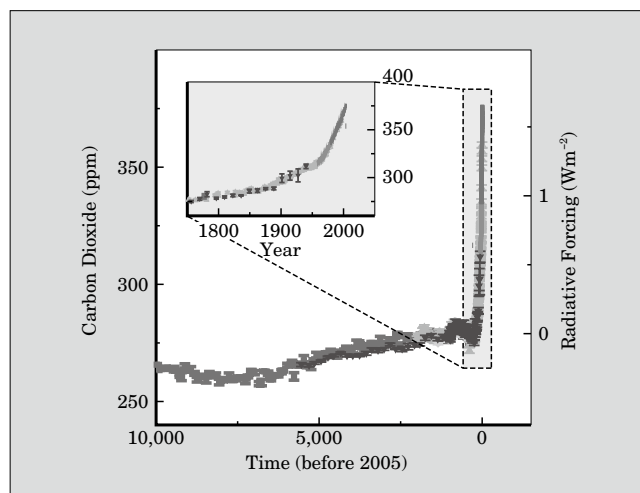
of the equipment, reduced maintenance, and a fewer number of protection components also contribute to resource conservation. Lower cost and an expanded product series and range of applications contribute to energy conservation through the expanded utilization of power-savings power electronics equipment.

This paper describes the present status and future outlook for Fuji Electric's representative power semiconductor products and focuses on power modules, power discretes and power ICs.

2. Power Modules

The most significant achievements for Fuji Electric's power modules in the past one year have been the technical development[3] of the "V-series" of 6th generation IGBTs (insulated gate bipolar transistors) and the use of the "U-series" of 5th generation IGBTs in the Toyota LEXUS[*1] models LS600h and LS600hL.

The V-series IGBT modules have further advanced the FS (field stop) and trench-gate structures that had been developed with the U-series. As a result, the chips are thinner and the carrier density distribution is improved, thus advancing the trends toward smaller chip size and lower loss. The design of the trench-gate structure utilizes a further evolved version of the noise reduction technology developed with the U4-series so that the chips realize lower loss, lower noise and a smaller size. The design of the package utilizes a thick copper layered DCB (direct copper bonding) substrate[4] to achieve higher reliability and to assure operation at 150 °C. Moreover, the internal wiring was designed in consideration of radiation noise generating mechanism that has been clarified through joint research with a university, and as a result a package is realized that is unlikely to emit noise. Figure 2 shows the trade-off relationship between radiation noise and loss measured by changing the gate resistance on a Fuji Electric test

---

*1: LEXUS is a registered trademark of Toyota Motor Corporation.

Fig.2 Relationship between radiation noise and loss
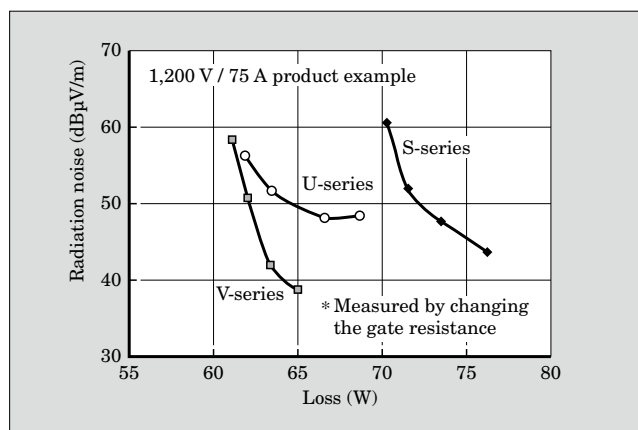
bench, and compares the V-series to other series. Despite its smaller size, the V-series achieves a 5 to 10% reduction in loss compared to the U-series at commonly used radiation noise levels. A product line is presently being developed and sample deployment for industrial applications has started in early 2008.

The PCU (power control unit) of the LEXUS LS600h and LS600hL maintains high reliability while achieving significantly lighter weight and higher output. Contributing to this lighter weight and higher output is Fuji Electric's IGBT chip technology that enables Denso Corporation's double-sided cooling technology for efficiently cooling the heat generated by power semiconductor devices and double-sided soldered mounting technology which achieves a high current density of 300 A per device. Figure 3 shows the power semiconductor peripheral configuration for the PCU of the LEXUS LS600hL. Fuji Electric's IGBT chip which improves upon the high current density specifications of the U-series and a FWD (free wheeling diode) chip are mounted onto the double-sided cooling power module made by Denso Corporation, and the double-sided cooling power module is sandwiched on both sides by a cooling tube and is assembled into a water-cooled power stack.

For both industrial applications and automotive applications, lower loss, smaller size and lower cost are strongly requested of power modules. With an eye toward further improvement in the future, Fuji Electric is developing high reliability and high heat radiating package technology, and at the same time is also researching and developing low loss MOS (metal-oxide-semiconductor) gated conduction modulation devices and FWD and SiC devices.

Fig.3 PCU for LEXUS LS600hL, double-sided cooling structure made by Denso, Ni/Au plated power chips made by Fuji Electric
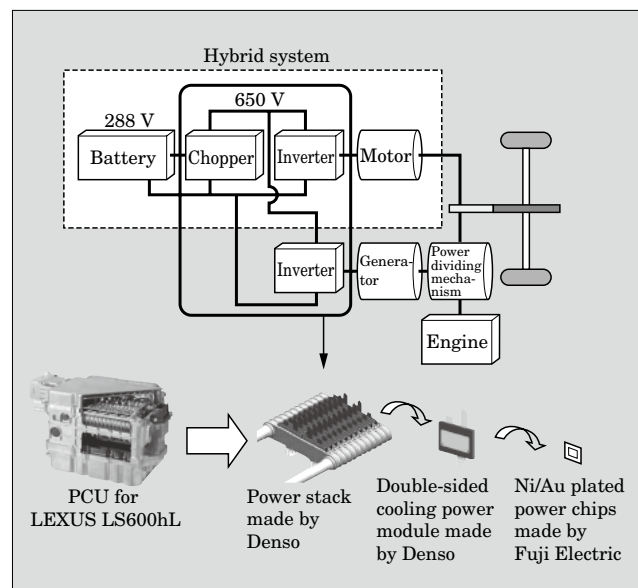
3. Power Discretes

Recent significant achievements for Fuji Electric's power discretes include the product launches of the SuperFAP-E³ series of 6th generation high-voltage MOSFETs (MOS field-effect transistors) and the SuperLLD3 series of 4th generation low-loss diodes.

The SuperFAP-E³ series further optimizes the quasi-plane-junction technology[5] developed with the 5th generation SuperFAP-G series to achieve an approximate 15% improvement in the figure of merit $R_{on} \cdot A$ that indicates low on-resistance and also optimizes the gate capacitance to realize both low loss and low noise. Figure 4 compares the SuperFAP-E³ series and SuperFAP-G series trade-off relationships between radiation noise and switching loss measured by changing the gate resistance on a Fuji Electric test bench. The SuperFAP-G series has low loss, but is sensitive to stray inductance, and is difficult to use because the layout on a printed circuit board requires care and attention in order to avoid voltage and current ringing. The SuperFAP-E³ series, in which the gate capacitance has been optimized, is built to be resistant to voltage and current ringing during switching even when the stray inductance is somewhat large. Without having to struggle with the layout on a printed circuit board, the user is able to design high efficiency switching-mode power supplies that comply with noise regulations and to reduce the number of noise-suppressing components.

The SuperLLD3 series, provided with a junction structure and drift layer design that have been improved compared to those of the conventional SuperLLD1 and SuperLLD2 series, realizes significantly lower loss. Figure 5 shows the importance of a low-loss diode by comparing the trade-off relationships between reverse recovery time and forward voltage drop for the SuperLLD3 and conventional series. Compared to the SuperLLD1 series in the same application to a continuous current mode power factor control circuit, the SuperLLD3 series has a forward voltage that is approximately 0.5 V lower, and a reverse recovery time that is approximately 25% shorter. The reduction in forward voltage leads to a reduction in conduction loss. The shorter reverse recovery time leads to a reduction of the diode's own switching loss and also contributes to a reduction in turn-on loss of the power MOSFET that is paired with the diode. Accordingly, use of the SuperLLD3 series is expected to be effective in reducing loss of the power factor control circuit as a whole. Furthermore, the low-loss diode for the power factor control circuit has already achieved lower noise in the conventional series, and the SuperLLD3 series is fabricated with the same low noise characteristics as those of the conventional series.

Power discretes are also strongly requested to provide lower loss, smaller size and lower cost while maintaining low noise performance, and research and

Fig.4 Trade-off relationship between radiation noise and switching loss
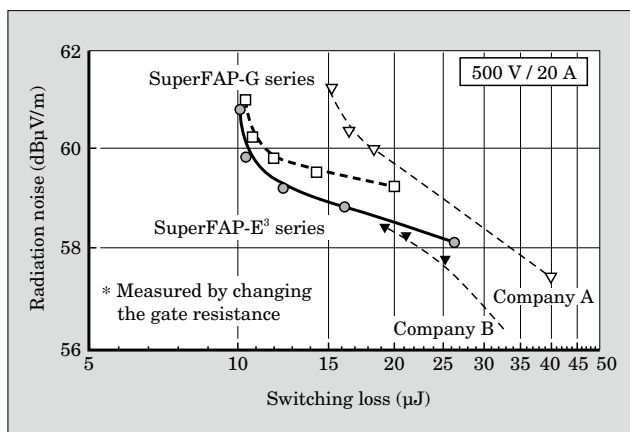
Fig.5 Trade-off relationship between reverse recovery time and forward voltage drop
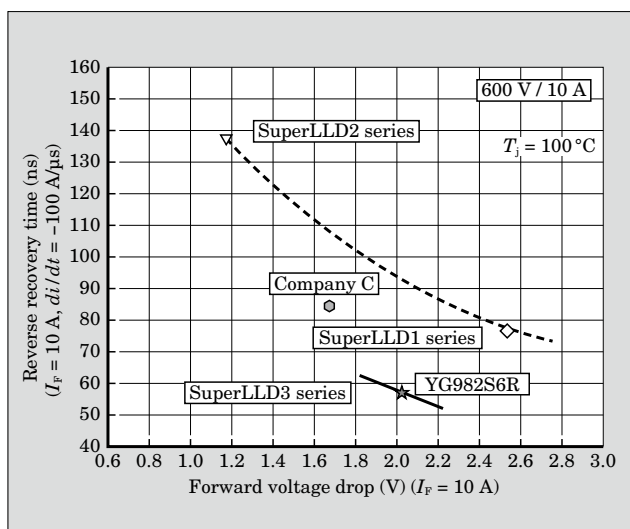
development activities are focused on satisfying these requests. Recently, the development of a 3rd generation trench MOSFET and of a SuperFAP-E³ 900 V series, and the expansion of the product lines of the SuperLLD3 series, a high-voltage SBD (Schottky barrier diode) series and a low I_r SBD series have been advanced with urgency. With an eye toward the future, research and development activities are advancing the technology for combining low on-resistance and low cost in a superjunction MOSFET[6].

4. Power ICs

Power ICs have realized many achievements as listed below.
(1) Mass-production of a Li-ion battery protection IC that integrates the world's first low on-resistance bidirectional power MOSFET[7], and use of this IC by a major Li-ion battery manufacturer
(2) Mass-production of the new M-Power 2 A series of high-efficiency low-noise power ICs for switch-

ing-mode power supplies, and their use by a major manufacturer of power supplies for LCDs (liquid crystal displays) televisions

(3) Mass-production of the FA5553/5547 series of multifunction low-standby-power PWM switching-mode power supply controller ICs

(4) Mass-production of the FA5550 series of switching-mode power supply controller ICs for continuous-current-mode PFC circuits

(5) Development of the FB8632J, 3rd generation micro DC-DC converter

(6) Mass-production of the FA7748/7749 series of DC-DC converter ICs for step-down rectification circuits

(7) Mass-production of a 5th generation 256-bit PDP (plasma display panel) address driver IC

(8) Mass-production of a 5th generation 96-bit PDP scan driver IC

(9) Mass-production of an IGBT driver IC for hybrid electric vehicles

(10) Mass-production of a single-chip low-noise ignitor for automobiles

(11) Mass-production of the F5052H miniature high-current IPS (intelligent power switch) for automobiles using COC (chip-on-chip) technology

Among these achievements, the Li-ion battery protection IC applies Fuji Electric's proprietary low on-resistance three-dimensional power device TLPM (trench lateral power MOSFET[7]) and is the world's first single-chip Li-ion battery protection IC provided with an integrated low on-resistance bidirectional MOSFET. Figure 6 shows the external appearance of this chip, an example of the chip mounted on a battery pack printed circuit board, a chip photograph, and a TLPM cross-sectional photograph. The integration into a single chip results in a smaller mounting area of 2.4 mm^2, which is less than 30% of the previously required mounting area, and contributes significantly to making thinner Li-ion battery packs, as well as thinner and smaller cell phones and other mobile electronic equipment.

As a high-efficiency, low-noise power IC for switching-mode power supplies, the M-Power 2 A series is a 3rd generation product that uses Fuji Electric's proprietary control technology to continue to enable the easy configuration of a current-resonance switching-mode power supply without concern for resonance shifting. Since high-efficiency and low-noise high-power switching-mode power supplies of up to 400 W can be configured easily, this IC is compatible with larger screen sizes of LCDs and flat panel televisions.

The 5th generation PDP address-driver IC supports the transition to 256-bit multi-bit implementations, and contributes to a reduction in panel cost by supporting LVDS (low voltage differential signal) and RSDS (reduced swing differential signal) input to decrease the number of signal lines. The 5th generation PDP scan-driver IC supports the transition to 96-bit multi-bit implementations, and achieves lower cost by improving SOI (silicon on insulator) technology and increasing the current density to reduce the area per bit while supporting full-HD (high definition) as a result of a higher breakdown voltage.

The micro DC-DC converter, as shown on the left side of Fig. 7, integrates an inductor, power MOSFET and controller IC in order to configure a DC-DC switching-mode power supply. Fuji Electric's proprietary inductor technology and chip-on-chip assembling technology[8] contribute to reducing the mounting area. Through circuit design innovations and optimized specifications, the 3rd generation micro DC-DC converter reduces the standby current and realizes an approximate 20% smaller size than the 2nd generation device. The right side of Fig. 7 compares the external appearance of the 3rd generation micro DC-DC converter with that of prior generations, and it can be seen that the size decreases steadily with successive generations of devices.

In order to reduce the loss and decrease the size of a power IC, lower loss and smaller size of the integrated output power device are the most important factors. Fuji Electric is vigorously advancing research and development into reducing the loss and decreasing the size of the integrated power devices in future power ICs[9][10]. For an even more distant future, Fuji Electric is researching the potential of digital control and is examining the possibility of converting existing analog control to digital control in order to realize higher precision control, smaller size and lower standby power.

Fig.6 Li-ion battery protection IC

(a) Appearance
(b) Example of IC mounted on a printed circuit board
Control circuit
Power MOSFET (TLPM)
(c) Chip
n+(S1) Gate n+(S2) n+(S1)
p base p base p base
n drain n drain
drain drain
(d) TLPM cross-section
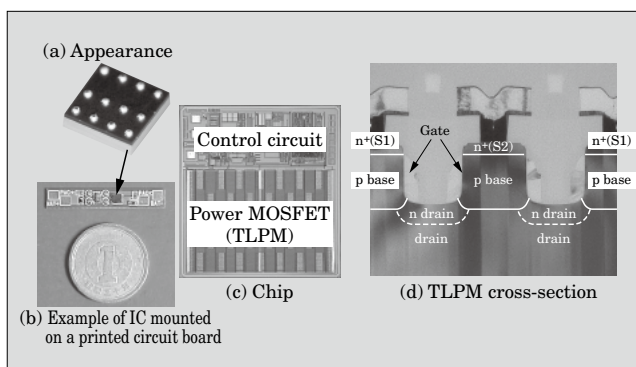
Fig.7 Appearance of 3rd generation micro DC-DC converter (comparison with conventional device)

Controller IC
MOSFET
SMD inductor
1st generation micro DC-DC converter
2nd generation micro DC-DC converter
3rd generation micro DC-DC converter
Conventional components for DC-DC converter (excluding capacitors)
0   3 mm
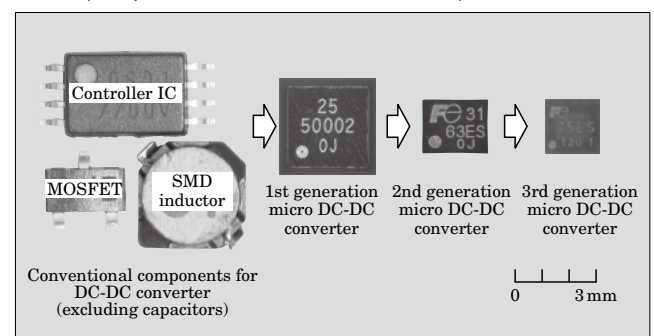
5. Pressure Sensors

Fuji Electric has completed the development of a 5th generation pressure sensor, and is moving ahead with preparations for mass-production. The 5th generation pressure sensor corresponds to a 2nd generation single-chip digital-trimming type pressure sensor. Compared to the 4th generation device, the designs of the diaphragm, digital-trimming circuit, operational amplifier, electromagnetic noise filter and surge protection circuit were optimized to achieve an approximate 30 % reduction in chip area. Pressure sensors are being used in increasing numbers in order to improve the fuel economy of automobiles and motorcycles, realize cleaner emission gas, improve safety, and also to increase the efficiency of industrial and residential air conditioners. Depending on the application, the precision of these pressure sensors is linked directly to improved fuel economy and efficiency. Therefore, pressure sensors are strongly requested to provide higher precision and lower costs, and with their expanding range of applications, compatibility with special environmental conditions is also being requested. In the future, Fuji Electric will continue to satisfy customer requests by improving our proprietary diaphragm technology and single-chip digital-trimming technology in order to achieve higher precision and lower costs and by developing products compatible with high-pressure and special environmental conditions.

6. Postscript

By innovating and promoting power electronics technology, Fuji Electric wants to help reducing CO_2 emissions, protect the global environment and contribute to sustainable development for human society. Power semiconductors are a key supporting element of this intention, and this paper has described chiefly the present status and future outlook for the main power semiconductor products.

For power semiconductors to contribute to reducing CO_2 emissions, protecting the global environment and achieving sustainable development for human society, the trends towards lower loss, lower noise, smaller size, higher reliability, lower cost, and expanding the product lineup and range of applications must progress at faster rates. On the other hand, quite a few technologies are thought to be approaching their theoretical limits, and future innovation is needed in the materials, process, device, circuit, package and test fields. Fuji Electric intends to put additional effort into technical development and intends to bolster efforts to cultivate personnel capable of creating technology and personnel capable of realizing technical innovation.

References

(1) Intergovernmental Panel on Climate Change. Summary for Policymakers. Fourth Assessment Report. 2007-06.

(2) Energy Information Administration, U.S. Department of Energy. International Energy Outlook 2007. 2007-05.

(3) Onozawa, Y. et al. Development of the next generation 1,200V trench-gate FS-IGBT featuring lower EMI noise and lower switching loss. Proceedings of ISPSD'07. 2007, p.13-16.

(4) Nishimura, Y. et al. Investigations of all lead free IGBT module structure with low thermal resistance and high reliability. Proceedings of ISPSD'06. 2006, p.249-252.

(5) Kobayashi, T. et al. High-Voltage Power MOSFET Reached Almost to the Silicon Limit. Proceedings of ISPSD'01. 2001, p.435-438.

(6) Fujihira, T. Theory of Semiconductor Superjunction Devices. Japan Journal of Applied Physics. vol. 36, 1997, p.6254-6262.

(7) Fujishima, N. et al. A High-Density Low On-Resistance Trench Lateral Power MOSFET With a Trench Bottom Source Contact. IEEE Transactions on Electron Devices. vol. 49, no. 8, 2002, p.1462-1468.

(8) Hayashi, Z. et al. High-Efficiency DC-DC Converter Chip-Size Module With Integrated Soft Ferrite. IEEE Trans. Magn. vol. 39, Issue 5, 2003, p.3068-3072.

(9) Matsunaga, S. et al. Low Gate Charge 20 V Class Trench-aligning Lateral Power MOSFET. Proceedings of ISPSD'06. 2006, p.329-332.

(10) Sumida, H. et al. 250 V-Class Lateral SOI Devices for Driving HDTV PDPs. Proceedings of ISPSD'07. 2007, p.229-232.

Plated Chip for Hybrid Vehicles

Seiji Momota
Hitoshi Abe
Takayasu Horasawa

1. Introduction

The automotive industry is implementing various efforts to reduce carbon dioxide emissions in order to help preventing global warming. As a result of the sudden rise in crude oil prices and the like, hybrid vehicles that use both a gasoline engine and an electric motor are becoming more popular in Japan and the USA. Systems having higher output power and a smaller size are needed to further popularize these hybrid vehicles.

Leveraging Fuji Electric's experience obtained with industrial-use IGBT (insulated gate bipolar transistor) modules, in May 2006, we realized an IGBT-IPM (intelligent power module) product which provides the guaranteed high reliability necessary for auto applications, and since then have supplied IGBT-IPMs for use in the boost converters of the LEXUS*1 GS450h and the like. Then we commercialized a power chip product for the PCU (power control unit) that is installed in the LEXUS LS600h and LEXUS LS600hL hybrid vehicles which came to market in May 2007.

This paper describes, as IGBT chip technology for realizing the above products, a plated electrode structure for chips suitable for high current density and double-sided cooling, and Fuji Electric's efforts to increase the reliability of those chips.

2. Challenges

Toyota Motor Corporation's Hybrid System II (THS-II) is characterized by the combination of an inverter that controls two motors (a motor and a generator) and a converter that boosts the battery voltage, so that higher motor output can be realized without using a high-voltage battery. The THS-II circuitry, as shown in Fig. 1, is configured from 14 arms of semiconductor switches. The number of power chips arranged in parallel will differ according to the individual output capacities of the motor, generator and boost converter, but many power chips are used in the PCU system overall.

*1: LEXUS is a registered trademark of Toyota Motor Corporation.

Fig.1 THS-II circuit diagram
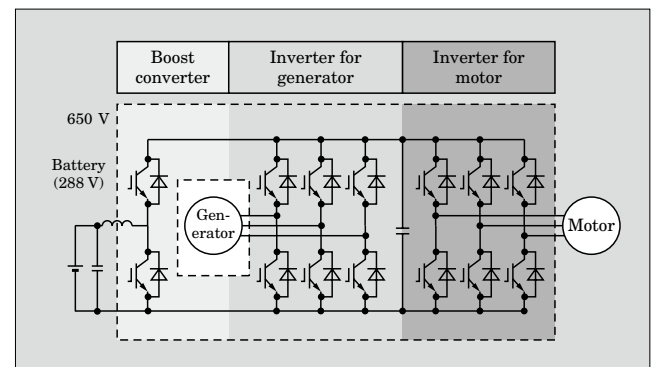
However, with this type of conventional module structure in which many power chips are arranged in a planar state, the PCU will have a large footprint, and the requirement for smaller size cannot be satisfied. Thus, it is important to reduce the number of power chips, and challenges for achieving this goal include developing a power chip capable of withstanding a high current density and achieving a significant improvement in heat dissipation performance.

3. Development Overview

The IGBT chip used in the LEXUS LS600h and LEXUS LS600hL applies the technology of an industrial-use 1,200 V FS (field stop) type trench gate IGBT[1] that Fuji Electric has been mass-producing since 2002. This IGBT has a structure that reduces the on-state dissipation and switching dissipation during power conversion, and an improved unit cell design for automotive-use so as to increase current density.

An aluminum layer is typically formed on the chip surface, and in the case of double-sided cooling, soldering is also required on the surface side. This is made possible by a Ni film which is formed by plating technology on the upper surface of an aluminum electrode.

Moreover, to guarantee the high reliability necessary for automotive applications, we improved the processing before and after the gate oxidation process, and to improve the sensing technology we enhanced the accuracy of the temperature sensing element and cur-

rent sensing element in the IGBT chip and developed a control IC.

4. Features
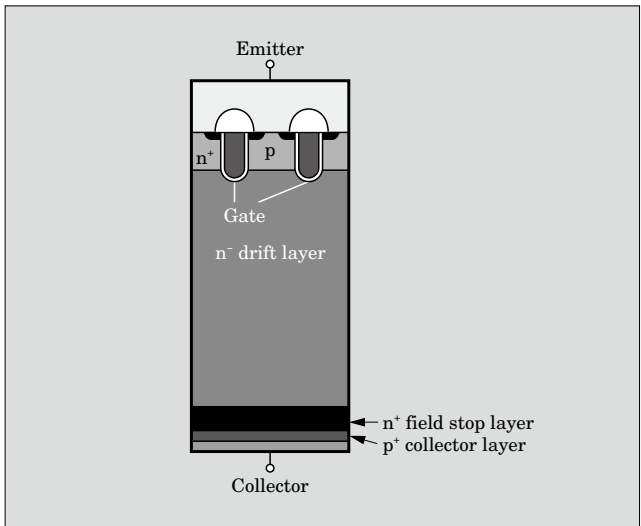
4.1 Improved chip characteristics

The IGBT chip is a voltage-driven switching semiconductor equipped with a MOS (metal-oxide-semiconductor) gate on its surface, and having voltage and current ratings higher than those of a bipolar transistor, exhibits highest performance as a 600 V or above high-voltage device. This device operates by repeating two states at high frequency, an ON mode that passes electric current and an OFF mode that maintains the voltage without passing electric current. The device was designed by improving the tradeoff relation between the different optimal structures for each of the variant operating states.

The FS-IGBT utilized herein employs a structure that achieves 1,200 V withstand voltage capability in an 140 μm thin chip, has a trench gate surface cell configuration, and maximally increases on-state characteristics to exhibit excellent performance. Figure 2 shows the unit cell cross-section of Fuji Electric's 1,200 V-IGBT.

The FS-IGBT requires a high level of manufacturing technology for grinding the semiconductor wafer thinly with high accuracy and for forming a diffusion layer on the wafer surface, and Fuji Electric, which has been involved in the development of thin wafer processing techniques from early on, is presently mass-producing wafer processed products with a 100 μm thickness.

Furthermore, with a total channel width increased to 1.5 times that of Fuji's prior chip, a reduction in saturation voltage and higher current density have been realized as shown in the I-V characteristic of Fig. 3. Moreover, a drive IC for sensing abnormal conditions in the FS-IGBT output and operating at high speed to protect the chip has been developed as a companion to

the FS-IGBT, and enables the practical utilization of a system that employs this high current density device.

Reliability testing verified that, under the severe conditions required for automotive applications, there is no change in device characteristics for these devices having higher current densities than in the past.

4.2 Plating technology

Even if a power device is able to operate with a high current density, cooling technology is also needed in order to use the device at its guaranteed operating temperature of $T_j = 150\,°C$ or less. In the past, aluminum film was usually formed on the surface of the IGBT and diode chip in order to bond an aluminum wire, and in such a case, cooling could only be implemented from the rear surface of the chip. Double-sided cooling requires a structure that can also be soldering on its surface side. Moreover, by providing a cooling structure on the chip surface, an abnormal increase in device surface temperature due to a short-circuit can be suppressed, and as a result, reliability is increased.

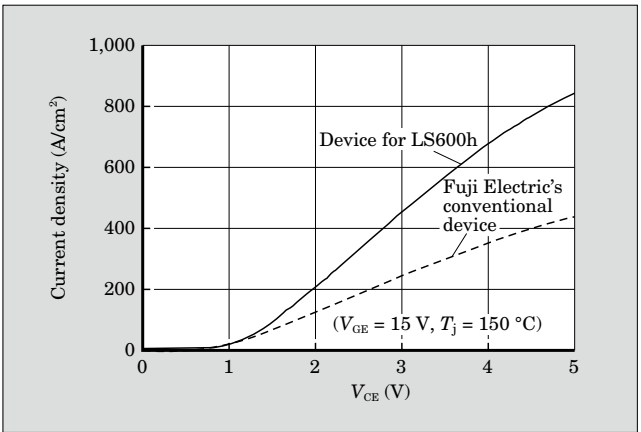Fig.3 Comparison of IGBT output characteristics
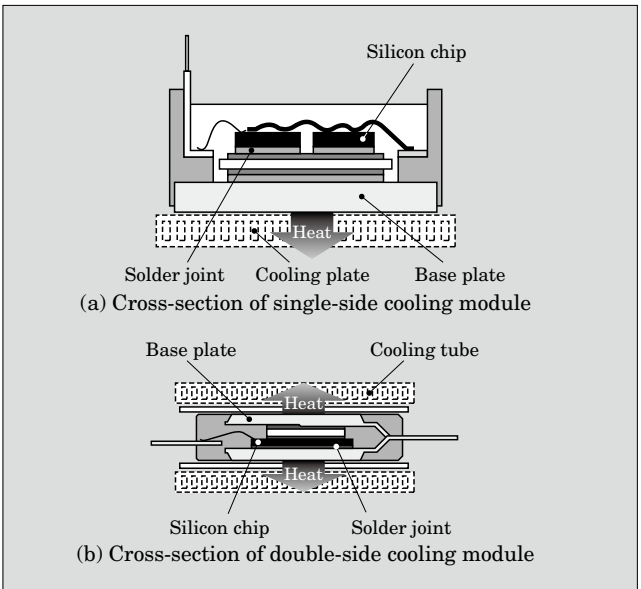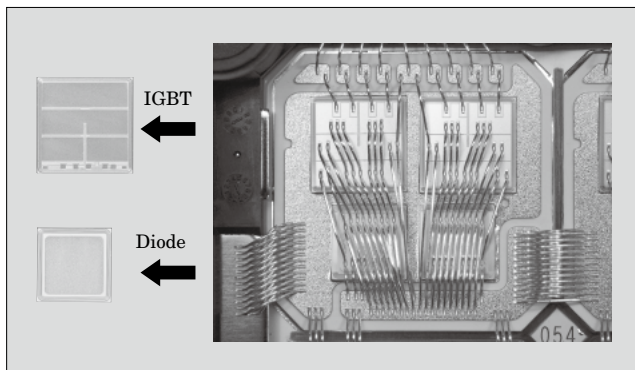

Fig.4 Comparison of cooling structures

(a) Cross-section of single-side cooling module

(b) Cross-section of double-side cooling module

Fig.2 IGBT unit cell cross-section

Fig.5 Chip comparison

Fig.6 Process flowchart including the plating process

This technique is also an effective means for shrinking the chip size[2]. Figure 4 shows a conventional module structure, and the internal structure of a double-sided cooling module made by Denso and for which IGBT and diode chip double-sided cooling is possible.

To enable the realization of this device, Ni film was plated over an aluminum electrode and Au film was plated on the surface to prevent oxidation. Figure 5 compares photographs of each chip. On the right side are an IGBT and a FWD chip in which wires have been attached to a conventional aluminum electrode, and on the left side is a chip whose surface has been plated with Ni and Au film.

The process flow of the plating process is shown in Fig. 6. After a device has been fabricated as usual, Ni plating and then Au plating are implemented consecutively to complete the chip.

The advantage of the plating method is that electrodes can be selectively attached only at locations where surface electrodes are exposed, differing for example from a method such as sputtering in which an electrode is attached to the entire surface, and hot etching and other processes can be eliminated. The technical challenges include preventing the plating material from wrapping around to the wafer rear surface and applying a plating film of uniform thickness to a wafer that may be warped due its thinness. Fuji Electric and Denso Corporation jointly developed technology to overcome these challenges and successfully commercialized the device.

4.3 Higher reliability

In contrast to industrial applications, since automotive applications have large load fluctuations and temperature fluctuations, and field accidents affect the human life, extremely high reliability and durability are required. In particular, the design and evaluation
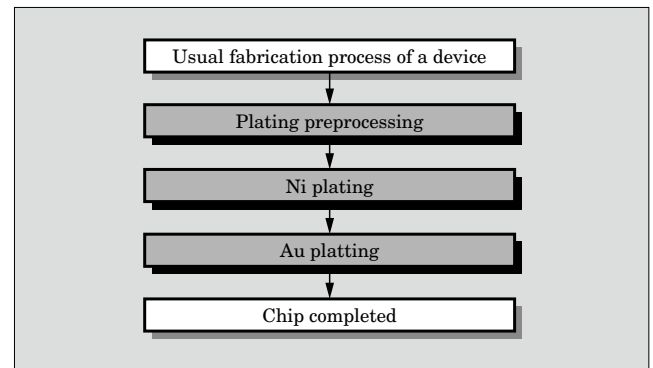
of this new device placed emphasis on the reliability of the gate oxidation film and the fluctuation of withstand voltage due to high temperature operation, which are important factors for IGBT chips. As a result, due to the improved processing before and after formation of the gate oxidation film and the reconsideration of the dimensions of the edge terminal structure, sufficient reliability for automotive applications was ensured.

Moreover, IGBT chips have been damaged when the temperature and current become excessive, and in order to utilize the maximum extent of the chip performance, protection techniques to prevent damage from occurring are important. Thus, a function for outputting the temperature and current is built into the IGBT chip, and measures were implemented to reduce the variances thereof. As a result, an abnormal state outputted from each sensing element can be sensed and protective measures implemented rapidly.

5. Postscript

A power semiconductor for use in the PCUs of hybrid vehicles has been developed. Aiming for the further popularization of hybrid vehicles in the future, efforts to reduce the costs of power semiconductors, batteries and motors will become increasingly important. Fuji Electric will continue to improve silicon devices, to develop devices that use new materials, and to contribute to the preservation of the global environment.

References
(1) Laska, T. et al. The Field Stop IGBT (FS IGBT) A new power device concept with a great improvement potential. Proc. 12th ISPSD. 2000, p.355-358.
(2) Otsuki, M. et al. Advanced thin wafer IGBTs with new thermal management solution. Proc. 15th ISPSD. 2003, p.144-147.

New IGBT-PIM with 6th Generation Chip and Package Technologies

Hayato Nakano
Yuichi Onozawa
Osamu Ikawa

1. Introduction

Power electronics, typically used for power control and conversion, have been utilized in a rapidly expanding range of applications in recent years. The main marketplace requirements for the latest power conversion system are small size, light weight and high efficiency. Therefore, technological improvements to power semiconductors are needed in order to achieve higher performance, more advanced functions and higher power handling capability.

One solution for system downsizing is to utilize an IGBT-PIM (power integrated module), in which an inverter circuit, a dynamic brake circuit and a rectifier diode are integrated all together in one module. The demand for PIMs has been increasing for several years because of their advantages of size and easy assembly, and because they provide an economical solution.

The next generation PIMs should have much smaller sizes and more economical features. The key to achieving high-performance compact PIMs is technology for reducing the silicon area while managing the electrical and thermal performance. The IGBT chip is undoubtedly the most important component in a PIM, and as such, must be designed with special consideration to exhibit the best performance. Because IGBT chips are the largest components and have the highest temperature in a module, a thermal management solution is always required. The development of both chip and packaging technologies is important for realizing high-performance compact PIMs, i.e., IGBTs should have be provided with improved power dissipation in a package having lower thermal impedance.

Another feature that new PIMs must exhibit is low noise radiation. The switching power dissipation can be classified as "static" and "dynamic" power dissipation. Static dissipation, which is related to the on-state voltage drop (V_{on}), depends slightly on the duty cycle, but is not strongly dependant on the driving condition. Dynamic dissipation, however, which integrates turn-on and turn-off energy, is significantly related to the driving condition.

2. New IGBT Chip Design Consideration

2.1 Performance challenges

The field stop structure, shown in Fig. 1, makes it possible to reduce the device thickness dramatically, which results in a significant performance improvement[1]. However, the turn-off oscillation issue that was observed in the Epi-type IGBT of the early 1990's has again become a potential problem. When the device becomes thin, it is easy to have "depletion layer reach-through" to the field-stop layer, which is the mechanism of the turn-off oscillation. The critical voltage of the oscillation should be outside of the SOA.

Thus, a breakthrough in the trade-off between the critical oscillation voltage and the breakdown voltage is needed in order to reduce device thickness. The critical voltage increases with lower-resistivity silicon, however the breakdown voltage decreases simultaneously.

The "ideal factor", shown in Fig. 2, is an important tool for understanding these criteria. The "ideal factor" is the ratio between the breakdown voltage of a real device and that of a theoretical plane junction with the same bulk resistivity and thickness. A 140 µm-thick FS-IGBT can be designed to only 70 % of the ideal factor in order to obtain oscillation-free turn-off, however, a 120 µm-thick device can achieve at least 86 % of the ideal factor without oscillation.

2.2 Easy *dv/dt* control

It is well known that an FWD having soft reverse recovery behavior is important for achieving lower turn-on dv/dt. However, there is little published work to report the importance of IGBT turn-on characteristics.

The planar gate-IGBT, which has enjoyed great popularity in the 20th century, has simple gate structures, and therefore its dynamic behavior is easy to predict based on physical dimensions. Trench IGBTs, however, have more variations and complexity in their gate structure, layout, and in optimization methods to compensate low V_{on} and provide a specific short-circuit capability.

Figure 3 shows an example of turn-on di/dt and dv/dt controllability with various gate resistances for

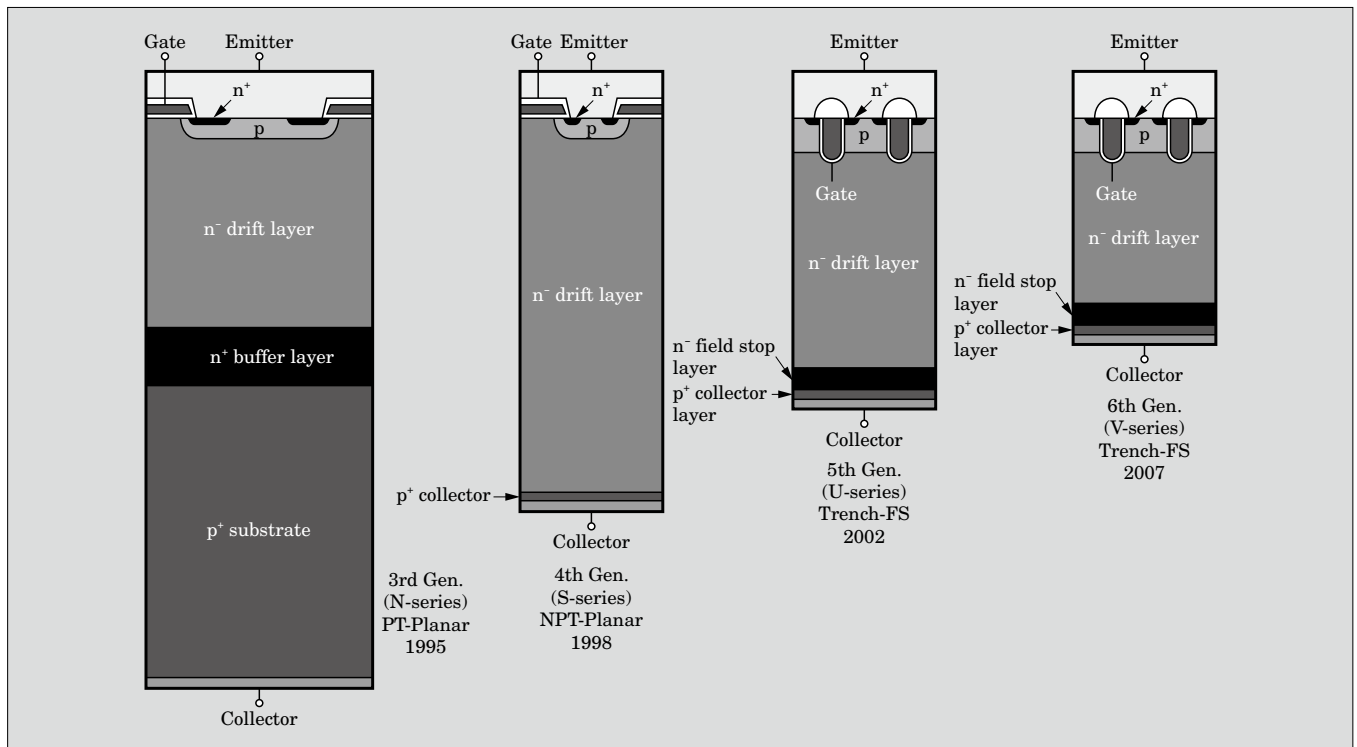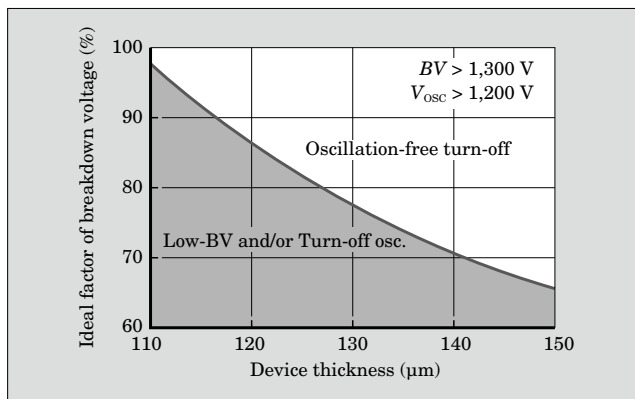Fig.1 Cross-sectional view of each generation of 1,200 V IGBT chips

Fig.2 "Ideal factor" required for oscillation-free turn-off FS-IGBT as a function of the device thickness

Fig.3 Small current turn-on *dv/dt* controllability with R_G for trench IGBTs with different gate designs

different trench gate designs. The turn-on current was 15 A, which is 1/5 of the rated current of 75 A. The gate resistance was varied from 7.7 Ω to 40 Ω. The FWD and IGBT were assembled separately on a special test piece to obtain only the effect of the IGBT design for the same FWD.

It is obvious that the turn-on behavior strongly depends on the trench design. Trench-A exhibits very little change in the switching waveforms versus gate resistance. Thus it is difficult to control dv/dt and di/dt with the gate resistance of this device. On the other hand, Trench-C shows outstanding controllability. The peak collector current, di_C/dt and dv_{AK}/dt can easily be controlled simply with a change in the gate resistance.

Hard switching behavior is often considered to be

caused by a poor design for FWDs. This is obviously correct, and hard reverse recovery FWDs are difficult to use with the new IGBT modules. However, in case of a trench-gate IGBT, it should be noted that turn-on be-

havior would be another cause of hard switching even though the FWDs are designed to have a soft recovery feature[2].

V-IGBT optimizations have been carried out with the following key goals[3].

(1) To realize a high "ideal factor" for both the main structure and junction termination

(2) To reduce the device thickness as much as possible while maintaining the oscillation-free turn-off performance

(3) To adjust the short-circuit current to have a consistent value and to maintain 10 μs-capability even at 150 °C

(4) To reduce the gate capacitance to the extent possible for fast switching

(5) To obtain consistent ruggedness and long-term reliability

3. Experimental Results

3.1 Static characteristics

After the device design was optimized, a 1,200 V-75 A V-IGBT and FWD chipset was experimentally evaluated. Figure 4 shows the J-V characteristics at room temperature and 125 °C, respectively, with a com-

parison to the current generation U-IGBT die. In order to make sure the improvement compared to the conventional device, the Y-axis is represented by current density. At a collector current density of 115 A/cm², a V_{on} of 1.7 V for the V-IGBT and 2.2 V for the U-IGBT, a reduction in V_{on} of up to 0.5 V has been achieved by optimizing the device structure and reducing the device thickness.

This great improvement in V_{on} clearly indicates the possibility of an increase in the rated current density while maintaining a lower V_{on} than in conventional devices.

3.2 Switching performance

Figure 5 shows a demonstration representing the improvement in the turn-off oscillation feature of a V-IGBT. The measurement conditions were: $V_{DC} = 1,250$ V, $I_C = 150$ A, $V_{GE} = +15$ V, -15 V and $T_j = 150$ °C. The figures clearly show that the V-IGBT has soft turn-off behavior with no oscillation even at extreme conditions. As a result of many measurements of turn-off oscillation at various ranges of DC-link voltage and temperature, it has been confirmed that no oscillation was found within the SOA guarantee.

Fig.4 J-V characteristics of a V-series IGBT

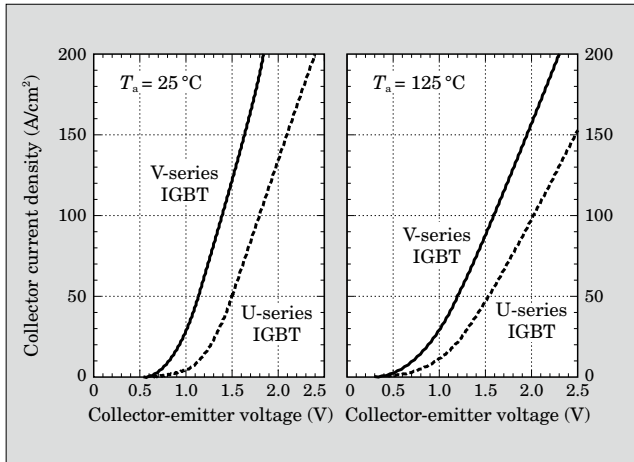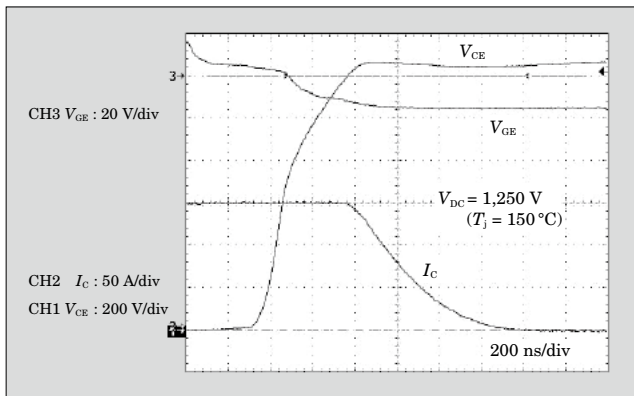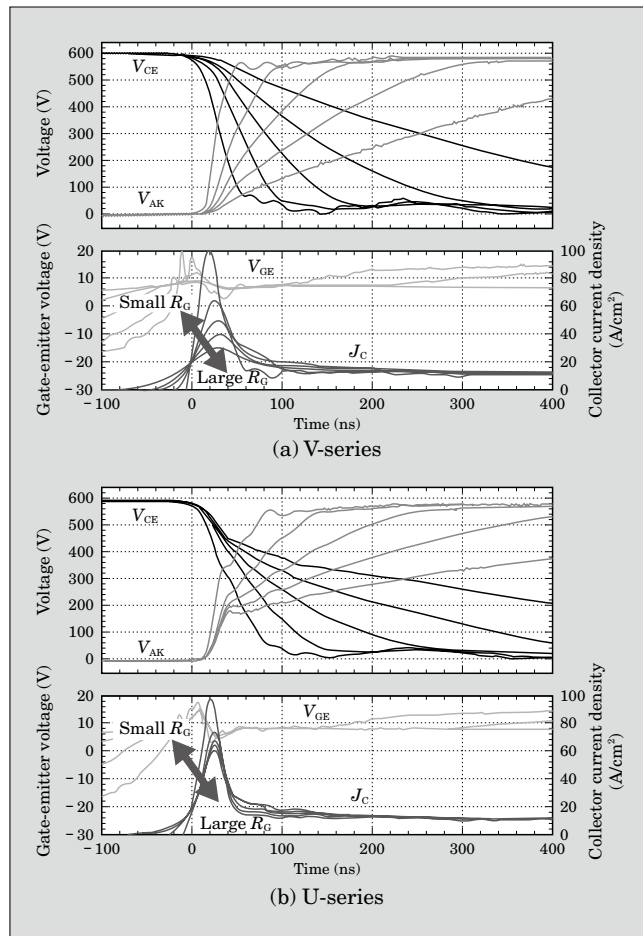Fig.5 Extreme measurement results demonstrating the turn-off oscillation $V_{DC} = 1,250$ V, $I_C = 150$ A

Fig.6 Comparison of small current turn-on behavior for different gate resistances

(a) V-series

(b) U-series

3.3 The "noise vs. switching loss" trade-off

The experimental results of the small current turn-on behavior of V-IGBTs and conventional IGBTs with various gate resistances are shown in Fig. 6. The measurement conditions were: $V_{CE} = 600$ V, $J_C = 11.7$ A/cm^2, $V_{GE} = +15$ V to -15 V and $T_j = $ R.T.

As mentioned earlier, the FWD dv_{AK}/dt corresponds to the IGBT turn-on di_C/dt. This means that with a new IGBT having excellent turn-on di_C/dt sensitivity to the gate resistance, control is much easier to implement in the FWD dv_{AK}/dt optimization process to compensate for noise radiation.
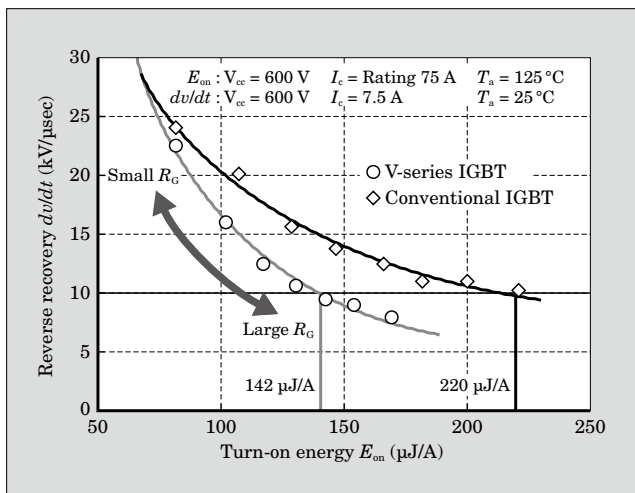
In addition, it is obvious from the figure that the V_{CE} waveforms strongly depend on the gate resistance. The higher the gate resistance is, the longer the voltage tail that appears in V_{CE} waveforms. These V_{CE} waveforms are observed not only for small current turn-on, but over the entire current range. Therefore, using an IGBT with poor di_C/dt controllability results in a greater penalty in E_{on}, in order to reduce noise.

Figure 7 shows the trade-off relationship between the FWD $dv_{AK}/dt_{(max)}$ at a small current (1/10 of rated current) and the IGBT E_{on} at a large current (rated current). The gate resistances were varied in the measurements. The measurement method used is the same as was used to create Fig. 3. The same FWD test piece was employed to isolate only the differences in the IGBT structure.

In case of the conventional IGBT, the turn-on energy of the large current is 220 µJ/A when the gate resistance is adjusted to the target dv_{AK}/dt at the small current turn-on of 10 kV/µs. On the other hand, the new large current IGBT has lower dv/dt characteristics over the entire range, and E_{on} at large current operation is a much lower value of 142 µJ/A, which is about a 36 % smaller E_{on}.

When measurements are started with a smaller gate resistance to find the target dv/dt by slightly in-

creasing R_G, V-IGBT will meet the target much faster than other IGBTs. This means fewer penalties in terms of switching loss in practical applications.

3.4 Ruggedness

One of the key features of the trench-FS IGBT is its high-temperature short-circuit capability. Figure 8 (a) shows the short-circuit measurement of V-IGBTs. Short-circuit gate pulses of +15 V, 10 µs width were applied to the gate at $V_{DC} = 800$ V and $T_j = 150$ °C. The device successfully turned off, because the V-IGBT has been designed during the device optimization stage to have a consistent short-circuit current.

Figure 8 (b) is an extreme demonstration of the device's ruggedness. The short-circuit measurement was performed with an intentionally large main inductance at 150 °C and a +15 V gate pulse of 8 µs width. No soft turn-off method was applied. The device survived the most critical condition of the self-clamping mode. This test also confirms that V-IGBTs have large switching current self-clamping capability.

3.5 Total power and temperature increase

It should be noted that it is very important to consider the rated current density of the new IGBTs while determining an optimum balance in terms of thermal management. In general, the smaller the silicon die size is, the higher the thermal impedance will be, and therefore, it is necessary to also achieve lower thermal impedance packaging technologies and combine them

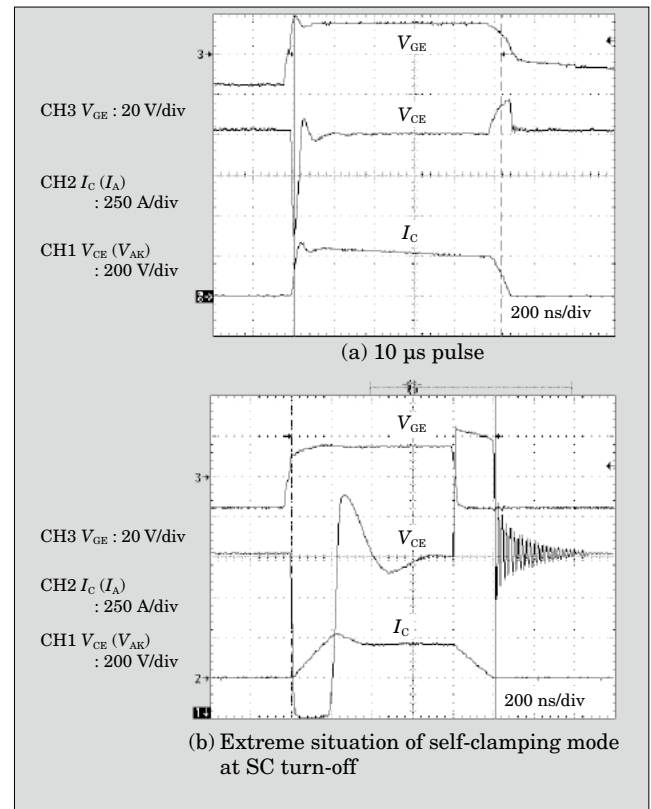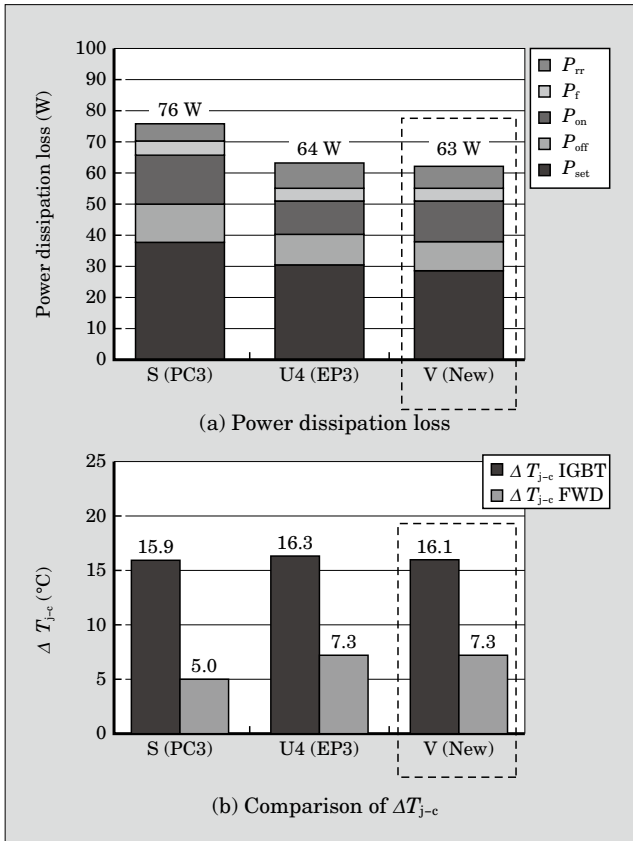Fig.8 Short-circuit demonstration of V-series IGBT at 150 °C

(a) 10 µs pulse

(b) Extreme situation of self-clamping mode at SC turn-off

Fig.7 Trade-off between small current $dv/dt_{(max)}$ and turn-on energy at rated current

Fig.9 Estimated total power and $\Delta T_{j\text{-}c}$ with adjusted R_G to obtain similar noise peaks

(a) Power dissipation loss

(b) Comparison of $\Delta T_{j\text{-}c}$

Fig.10 Product current rating by module size of Fuji's IGBT-PIMs

of the module power capacity. Figure 10 shows the 1,200 V PIM line-up listed by module type and rated current. The new product will have the same footprint size as the EP2 package up to 1,200 V-50 A. For the EP3-compatible physical size, a significant increase in current range has been achieved. 1,200 V PIMs of 100 A and 150 A rated current are available with the Fuji V-series of IGBT PIMs.
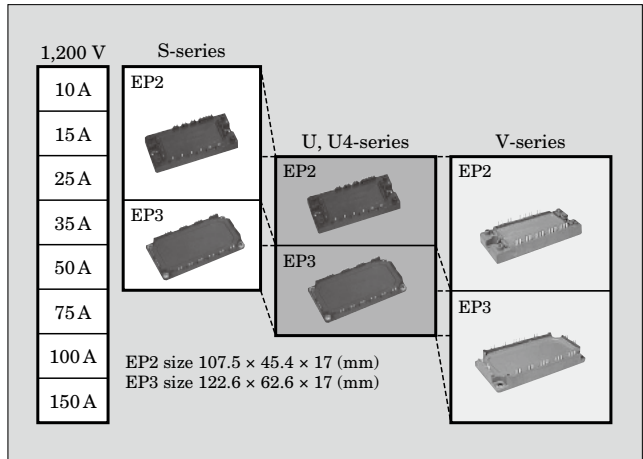
with techniques for shrinking the silicon die.

Figure 9 shows the estimated power dissipation and ΔT_j in a typical overdrive condition of a motor application. The gate resistances were experimentally selected so that these chip sets had similar FWD dv/dt at low current turn-on. It is clear from the figure that the total power dissipation of the V-series is 63 W, which is very similar to the 64 W power dissipation of the U4-series. An estimate of the temperature rise is also available, as shown in Fig. 9 (b). The $\Delta T_{j\text{-}c}$ of the IGBT is 16.1 °C for the V-series, which is very similar to that of former generation modules.

4. Product Line-up

Compared to the S-series and U4-series, V-series PIMs have a smaller IGBT die size. The impact of these results is directly apparent in the enhancement

5. Postscript

Fuji V-series IGBT PIMs have been presented in this paper. The 6th generation chip has made it possible to realize IGBT PIMs having "low noise radiation," "compact size" and "high performance." The PIM power range has been extended up to 1,200 V-150 A with an EP3-compatible size package. Fuji's new PIMs are helping to provide more effective and economical solutions of power electronics.

References
(1) Laska. T. et al. The Field Stop IGBT (FS IGBT) – A new power device concept with a great improvement potential. Proc. ISPSD 2000. p.355-358.
(2) Nemoto. M. et al. An Advanced FWD Design Concept with Superior Soft Reverse Recovery Characteristics. Proc. ISPSD 2000. p.119-122.
(3) Otsuki. M. et al. Investigation on the short-circuit capability of 1,200V trench gate field-stop IGBTs. Proc. ISPSD 2002. p.281-284.

5th Generation Digital Trimming Type Automotive Pressure Sensors

Kazunori Saito
Mutsuo Nishikawa
Kimihiro Ashino

1. Introduction

The automotive industry's environmental activities are increasing at the same time as environmental regulations in Europe, United States, Japan, Asia and elsewhere throughout the world are being strengthened. To comply with such regulations, the systems used in automobiles are day-by-day becoming more efficient and are achieving higher control accuracy. Moreover, engine management that measures pressure and performs control is becoming increasingly important in these systems.

Fuji Electric began mass-producing automotive pressure sensors in 1984. In response to strict cost requirements and changes in the required accuracy, Fuji Electric has developed proprietary high reliability circuit technology and advanced MEMS (micro electro mechanical systems) technology to be used in Japanese and overseas models of automobiles and motorcycles, and since 2002, has been mass-producing automotive pressure sensors with digital trimming using a 4th generation CMOS (complementary metal-oxide-semiconductor) process.

A 5th generation digital trimming type automotive compact pressure sensor (hereafter referred to as the 5th generation pressure sensor) that maintains the equivalent features, performance (output accuracy) and EMC (electromagnetic compatibility) protection performance as the 4th generation digital trimming type automotive pressure sensor, while achieving a more compact size, has been developed and is introduced herein.

2. Pressure Sensor Applications in Automobiles

Figure 1 shows pressure sensor applications in automobiles. The electronic fuel injection system of an engine contains a MAP (manifold absolute pressure sensor) and a TMAP (temperature manifold absolute pressure sensor) that measure intake pressure, and in order to promote further widespread use of these fuel injection systems, and even apply them to motorcycles, requests for lower cost and smaller size sensors are accelerating. Pressure sensors are also used in sensing filter clogging of the AFB (air filter box) in an intake

Fig.1 Applications of automotive pressure sensors
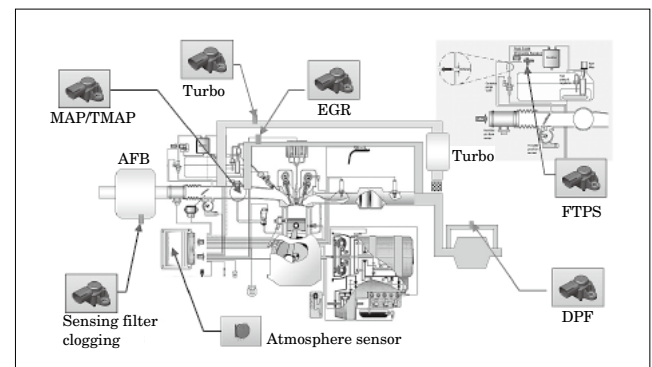
system and the DPF (diesel particulate filter) in an exhaust system, in a turbo pressure system that reuses exhaust gas, and in an EGR (exhaust gas recirculation) system. Pressure sensors are also used in atmospheric pressure sensors for high altitude compensating when an automobile travels at a high altitude, and in FTPS (fuel tank pressure sensors) to comply with regulations that have been enacted in Europe and South Korea for sensing leakage from a fuel tank.

3. Development History of Fuji Electric's Pressure Sensors

The development roadmap of Fuji Electric's automotive pressure sensors is shown in Fig. 2. In 1984, Fuji released a 1st generation pressure sensor, mainly for engine control in automobiles, which incorporated amplifier technology using bipolar ICs and surge protection. Thereafter, Fuji released 2nd and 3rd generation devices adopting one-chip and thin film trimming technology, and with the 4th generation, began mass-producing the world's first single-chip digital trimming type automotive pressure sensor that uses a CMOS process.

In order to satisfy the market demands for both low cost and high reliability, Fuji Electric has newly developed a 5th generation pressure sensor that carries on the "all in one chip" basic concept and maintains the functions, performance and EMC protection of the 4th generation device, while achieving a smaller size.

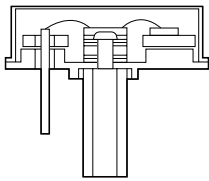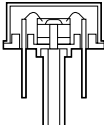Fig.2 Development roadmap of Fuji Electric's automotive pressure sensors

Sensor technology	1985	1990	1995	2000	2005	2010
	1st gen.		2nd gen.	3rd gen.	4th gen.	5th gen.	6th gen.
IC process	Bipolar				CMOS	
Trimming	Thin film trimming		On-chip thin film trimming		CMOS digital trimming	
Chip function	Diaphragm etching (wet → dry)					
	Piezo resistance (diffused resistance)					
	AuSn solder junction of Si+Si base		Chip electrostatic junction	Chip junction vacuum chamber	Vacuum chamber wafer electrostatic junction	
MEMS technology — Mechanical function / Electrical function			Bipolar amp		CMOS amp	High accuracy CMOS amp
			Thin film		Digital trimming + DAC	
				EMC protective device		High density EMC protective device
						Temperature sensor
						Exhaust gas resistant

Fig.3 5th generation pressure sensor and 4th generation pressure sensor

(a) 5th generation   (b) 4th generation

Fig.4 Example of diaphragm optimization by FEM analysis
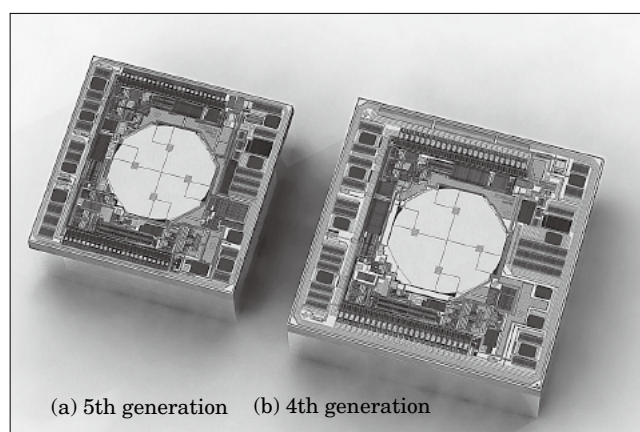
4. Characteristics

Figure 3 compares the newly developed 5th generation pressure sensor to the 4th generation pressure sensor.

The 5th generation pressure sensor realizes the equivalent functionality and performance as the 4th generation pressure sensor, and its main characteristic is a reduction in size, achieved through optimization and limit design, to 70% that of the 4th generation device.

The optimized design used in the 5th generation pressure sensor is described below.

4.1 Diaphragm design

FEM (finite-element method) analysis was used to design and optimize the diaphragm that forms the sensor part.

Figure 4 shows an example of this analysis. By modeling the cross-sectional shape of the diaphragm, the amount of displacement when pressure is applied and the stress generated on the chip are calculated, and additionally, the sensitivity and non-linearity of the sensor output are computed, and the optimal points for these parameters are obtained. As a result, the diaphragm area is reduced without decreasing sensor sensitivity and non-linearity, and performance equivalent to that of the 4th generation sensor is realized.

Fig.5 5th generation pressure sensor circuit block diagram
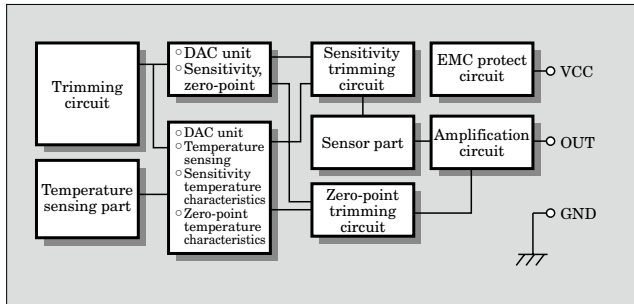
Table 1 Circuit block area ratios (compared to the 4th generation)

Circuit block		Area ratio
Sensor part	(IC pattern surface)	80%
Digital part	Trimming circuit part	70%
Analog part	D-A converter part	55 to 80%
	Temperature sensing part	100%
	Sensitivity trimming circuit	100%
	Zero-point trimming	100%
	Amplification circuit	100%
EMC, etc.	EMC protect circuit	60%
	Surge protection device	70 to 125%

Table 2 Noise resistant and surge resistant performance

| Item		Performance
ESD	MM (0 Ω, 200 pF)	Analog : ±1 kV or more Digital : ±600 V or more
	HBM(1.5 kΩ, 100 pF)	±8 kV or more
ISO7637	Pulse1, 2, 3a, 3b	Satisfies level-IV
Impulse		±1 kV or more
Latch-up	Current injection	±500 mA or more
EMS (G-TEM)	100 V/m	Fluctuation : 1% of FS or less
Over voltage	Between VCC and GND	16.5 V
Wrong connection	Between VCC and GND	5 V / 0.3 A

Also at this time, the effect of stress, which has been generated at the diaphragm, acting on the circuit part (area other than the diaphragm) is assessed, and accordingly, the distance from the sensing part on the diaphragm to the circuit area (margin) is minimized, which leads to a reduction in area.

4.2 Circuit and layout design

The circuit block configuration of the 5th genera-

tion pressure sensor is shown in Fig. 5. This configuration is entirely the same as that of the 4th generation pressure sensor, and no functions or blocks have been removed.

Based on the successful track record of the 4th generation device, we reevaluated Fuji Electric's proprietary design rules for vehicle sensors to achieve greater miniaturization with higher integration, and were able to reduce the size of each part of the chip as shown in Table 1.

However, we did not reduce the size of the analog part, and in particular the amplification circuit, the sensitivity trimming circuit, the zero-point trimming circuit and the temperature sensing part, which is directly linked to output accuracy.

As a result, the functions, performance and trimming range were maintained as equivalent to those of the 4th generation device.

4.3 Noise resistant and surge resistant design

A design that is both noise and surge resistant is increasingly being requested so that an automobile does not malfunction when traveling in an area of strong electromagnetic waves or in an electrically or magnetically severe environment.

In the 5th generation pressure sensors which satisfy these requests, while the chip size was being reduced, some chip areas were enlarged to accommodate protection devices, and the chip design placed an emphasis on noise resistance and surge resistance.

The result, as shown in Table 2 for the ESD (electrostatic discharge) machine model (0 Ω/200 pF), verifies tolerated voltage of ±600 V or more and the highest level of noise resistance and surge resistance by a single chip for automobile applications.

5. Postscript

An overview of the 5th generation digital trimming type automotive compact pressure sensor has been presented. With products being broadly developed for Japan and overseas, the accuracy, quality and cost requirements of pressure sensors are expected to become even more severe in the future. Fuji Electric intends to advance technical development for higher accuracy and higher quality products, and also to push forward with the development of products that are essential to the market.

SuperLLD3 Series of 600 V Low-loss Fast-recovery Diodes

Tetsuhiro Morimoto
Taketo Watashima
Masaki Ichinose

1. Introduction

At present, societal problems such as global warming and environmental disruption are diverse, and the conservation of resources is often called for. Reducing power consumption, increasing efficiency and simplifying the circuitry to achieve a smaller size and fewer components are important considerations for electronic equipment. Also, the switching power supplies installed in electronic equipment are advancing toward lower power consumption, higher efficiency, higher frequency, and lower noise emission.

Fuji Electric has commercialized and developed a product line of various diodes, including low-loss fast-recovery diodes (LLD) and Schottky barrier diodes (SBD), as rectifying diodes suitable for various applications to power supplies.

This paper presents an overview of the newly developed SuperLLD3 series of 600 V low-loss fast-recovery diodes intended for use primarily in power factor correction in switching power supplies. (See Fig. 1.)

2. Suitable Applications and Requirements of the SuperLLD3 Series

In electronic equipment that uses commercial power supplies, a rectification circuit for AC-DC conversion

Fig.1 Exterior view of SuperLLD3 series of 600 V low-loss fast-recovery diodes

is often utilized in the input rectification part. This circuit generates a distorted current waveform and is the source of harmonic component current, causing such problems as malfunction and decreased longevity of the electronic equipment and a lower power factor of the supplied power. Meanwhile, legal regulations in each country mandate the suppression of harmonic components, and a power factor correction circuit is added to comply with these regulations. As described above, the trend toward higher efficiency of power supplies is intensifying, and therefore a power factor correction circuit is absolutely essential for achieving higher efficiency and lower power loss in the system overall. The power factor correction circuit has a circuit configuration as shown in Fig. 2, and uses either a non-continuous inductance current method (current discontinuous mode) or a continuous inductance current method (current continuous mode) as the control method. Of these control methods, the current continuous mode is used mainly for high output power supplies. With this method, since the MOSFET (metal-oxide-semiconductor field-effect transistor) is made to ON during forward conduction of the diode, the forward current of the diode will be forcibly reverse-biased, and the problem of suppression of switching loss that accompanies the reverse recovery phenomenon of a diode must be considered.

Moreover, suppression of the forward loss of a diode must also be considered in order to increase the output and reduce the size of a power supply. Accordingly, in addition to reducing the reverse recovery time (t_{rr}), it is also important to reduce the forward voltage (V_F) of a diode. Thus, a LLD is needed that achieves higher speed than Fuji Electric's conventional SuperLLD1 series specialized for high-speed (short t_{rr}) and also has a lower V_F.

Figure 3 shows an example of the loss analysis results of a diode and MOSFET in a current continuous mode power factor correction circuit. The MOSFET accounts for two-thirds of the total loss, which is an extremely large percentage, and the turn-on loss which accounts for approximately half of this loss is largely affected by the reverse recovery characteristics of a diode. Thus, a diode that is higher speed and achieves a
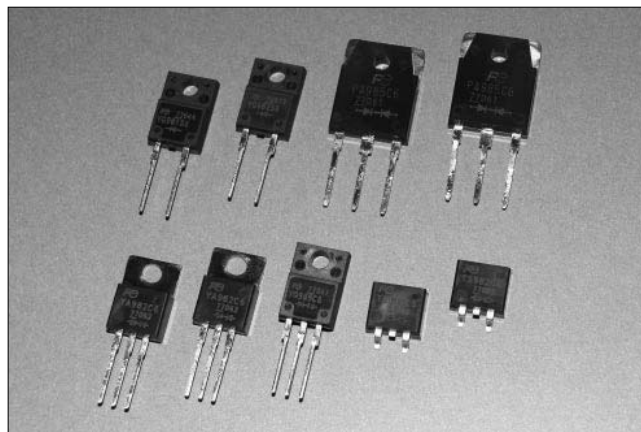
Fig.2 Power factor correction circuit and operation waveforms

(a) Power factor correction circuit

∗ L_a is the wiring interface.

(b) Waveform for inductance current continuous mode

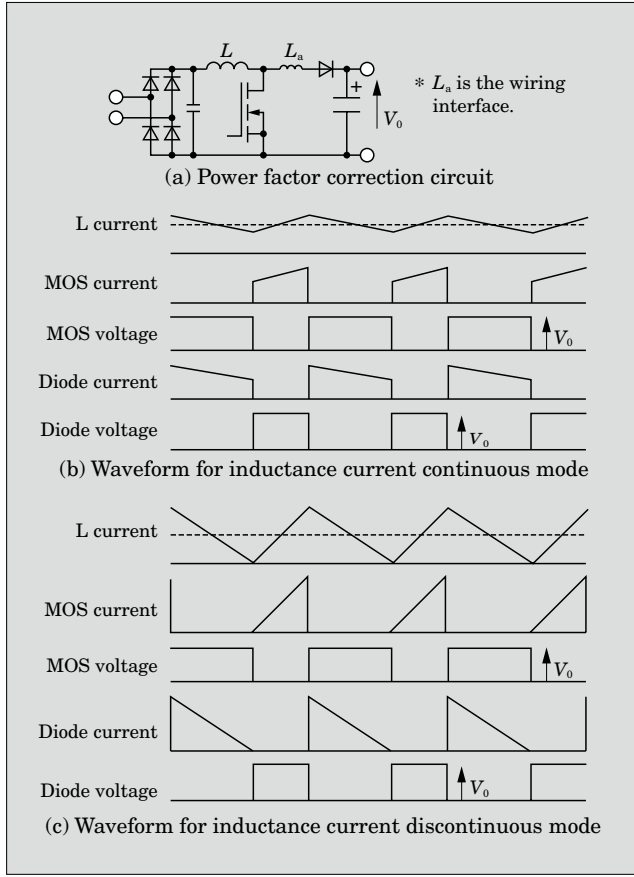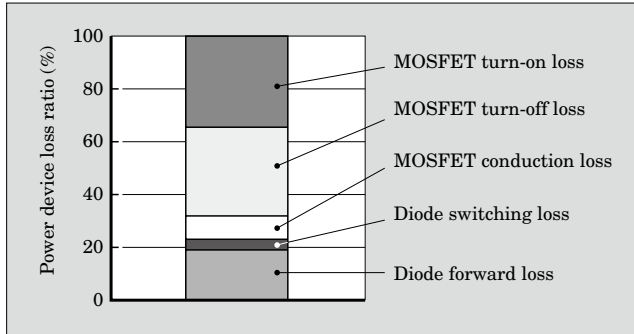(c) Waveform for inductance current discontinuous mode

Fig.3 Simulation of loss generated in power devices of current continuous mode power factor correction circuit

- MOSFET turn-on loss
- MOSFET turn-off loss
- MOSFET conduction loss
- Diode switching loss
- Diode forward loss

lower V_F than Fuji Electric's conventional SuperLLD1 device is needed in order to reduce the MOSFET turn-on loss. The newly developed SuperLLD3 realizes a 25% shorter t_{rr} and a 20% lower V_F than the SuperLLD1.

3. SuperLLD3 characteristics and application example

The V_F-t_{rr} trade-off correlation of the newly developed SuperLLD3 and the conventional SuperLLD1 and SuperLLD2 are compared for 10 A devices as shown in Fig. 4. The SuperLLD3 is significantly improved compared to the V_F-t_{rr} trade-off line of the SuperLLD1

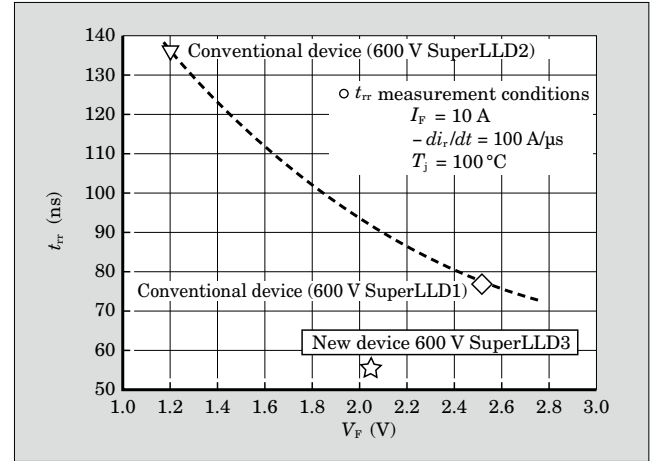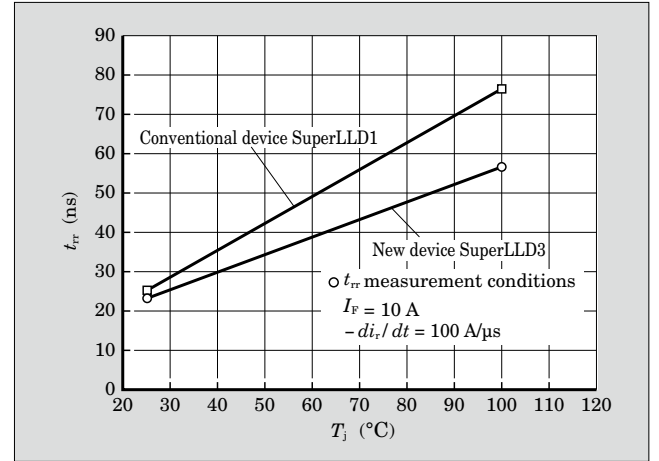Fig.4 V_F-t_{rr} trade-off correlation

Fig.5 t_{rr} temperature dependence

and SuperLLD2. The reverse recovery time t_{rr} is suppressed by approximately 25% compared to the SuperLLD1, and this is effecting in reducing switching loss during high frequency operation.

Next, Fig. 5 shows the temperature dependence of trr. With the SuperLLD3, the t_{rr} temperature change rate is smaller than for the SuperLLD1, and thus for high temperature operation, the switching loss is considered to be less temperature dependent.

Figure 6 shows the results of a comparison of the forward characteristics of the SuperLLD3 and the SuperLLD1. The SuperLLD3 has forward characteristics that are approximately 20% lower than the SuperLLD1 at high temperature (100 °C), thereby enabling a reduction in forward loss. Table 1 shows the results of comparing the characteristics of the SuperLLD3 and the SuperLLD1. Next, in order to verify the effect of the SuperLLD3 that achieves higher speed operation and lower V_F, an evaluation was carried out with an actual current continuous mode power factor correction circuit. The evaluated power supply had an output of 390 W (390 V/1 A) and the switching frequency was 65 kHz.

Table 2 shows the measured temperature rise and

conversion efficiency of the diode and MOSFET when mounted in the SuperLLD3 and SuperLLD1, respectively. The diode and MOSFET were evaluated using separated heat sinks. Due to a significantly lower V_F and a higher speed t_{rr}, the temperature rise of the diode mounted on the SuperLLD3 was approximately 11 °C lower than in the case of the SuperLLD1. Moreover, the MOSFET's drain current, which affects the turn-on loss that accounts for approximately one-third of the

loss, is reduced due to application of the SuperLLD3, and thus the temperature rise of the MOSFET was also suppressed. Application of the SuperLLD3 enables a reduction in the total temperature rise of the diode and MOSFET, and an approximate 1% improvement in conversion efficiency.

4. SuperLLD3 Design Measures[(1)]

Figure 7 shows the basic structure of a planar type diode. The LLD uses a lifetime killer diffusion process to achieve higher speed operation.

As an example of LLD design considerations, Fig. 8 shows the correlation between V_F and t_{rr} at

Fig. 6 Comparison of 600 V 10 A LLD forward characteristics

Fig.7 Cross-section of LLD chip

Fig.8 V_F-t_{rr} trade-off correlation

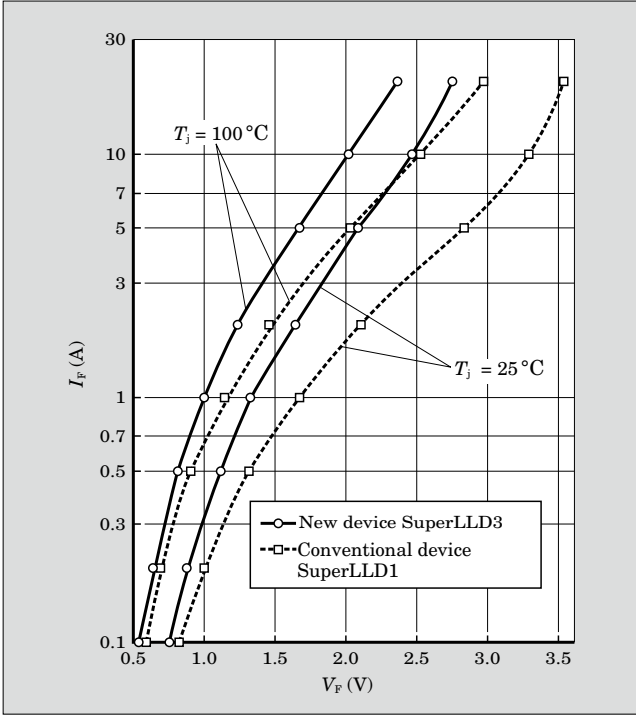(a) Experiment 1

(b) Experiment 2

Table 1 Comparison of SuperLLD3 and SuperLLD1 characteristics (actual measured values)

Item	Condition		New device SuperLLD3	Conventional device SuperLLD1	Units
V_F	25 °C	I_F = 10 A	2.5	3.3	V
	100 °C		2.0	2.5	V
t_{rr}	25 °C	I_F = 10 A $-di_r/dt$ = 100 A/µs	23	25	ns
	100 °C		57	77	ns
I_{RP}	25 °C		1.2	1.2	A
	100 °C		1.75	1.74	A

Table 2 Temperature rise and efficiency of SuperLLD3 and SuperLLD1

Item		New device SuperLLD3	Conventional device SuperLLD1	Units
Efficiency		88.16	87.17	%
Temperature rise of case	Diode	35.7	46.8	°C
	MOSFET	50.4	52.9	°C

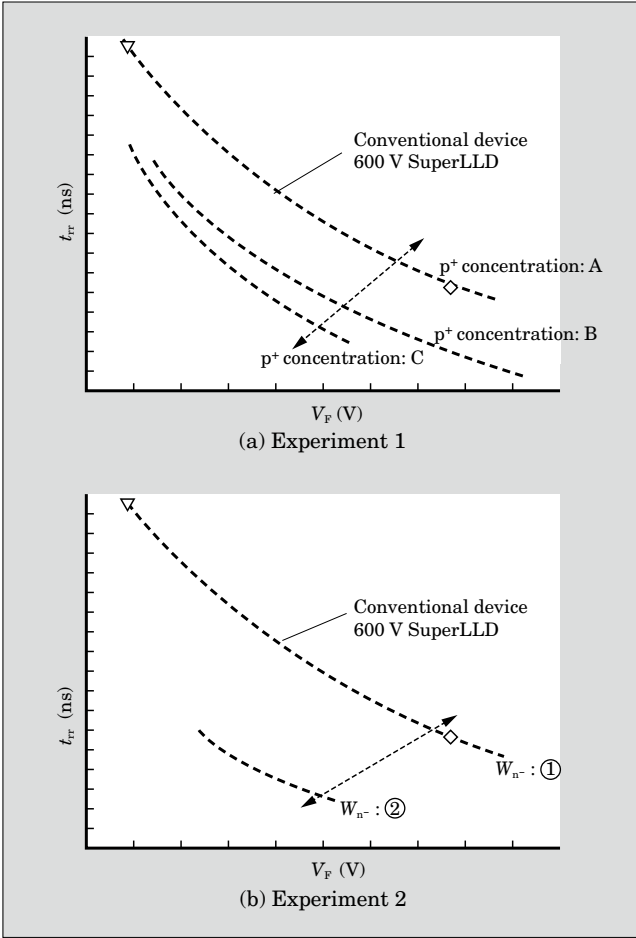Conditions: 390 W (390 V, 1.0 A output), 65 kHz

Table 3　600 V SuperLLD3 absolute maximum ratings and electrical characteristics

Device type	Package	Chip composition	Absolute maximum ratings			Electrical characteristics				
			V_{RRM} (V)	$I_{o\,(max)}$ (A)	I_{FSM} (A)	V_{FM} (V) (T_j = 25 °C)		I_{RRM} (µA) $V_R = V_{RRM}$	t_{rr} (ns) I_F = 0.1 A, I_R = 0.2 A, I_{rec} = 0.05 A	$R_{th\,(j-c)}$ (°C / W)
YA981S6R	TO-220AB	Single	600	8	40	3.0	I_F = 8 A	25	26	2.50
YG981S6R	TO-220F	Single	600	8	40	3.0	I_F = 8 A	25	26	4.50
TS982C6R	T-pack (S)	Twin	600	16	40	3.0	I_F = 8 A	25	26	1.50
YA982C6R	TO-220AB	Twin	600	16	40	3.0	I_F = 8 A	25	26	1.50
YG982C6R	TO-220F	Twin	600	16	40	3.0	I_F = 8 A	25	26	2.00
YA982S6R	TO-220AB	Single	600	10	50	3.0	I_F = 10 A	30	28	2.00
YG982S6R	TO-220F	Single	600	10	50	3.0	I_F = 10 A	30	28	3.50
TS985C6R	T-pack (S)	Twin	600	20	50	3.0	I_F = 10 A	30	28	1.25
YA985C6R	TO-220AB	Twin	600	20	50	3.0	I_F = 10 A	30	28	1.25
YG985C6R	TO-220F	Twin	600	20	50	3.0	I_F = 10 A	30	28	1.75
PA985C6R	TO-3P	Twin	600	20	50	3.0	I_F = 10 A	30	28	1.50

100 °C when the densities of three types of p^+ layers (A < B < C) and the lifetime killer diffusion density were varied. Similarly, the figure also shows the correlation between V_F and t_{rr} at 100 °C when the thicknesses of two types of n^- layers (① > ②) and the lifetime killer diffusion density were varied. From Fig. 9, it can be seen that by increasing the densities of the p^+ layers and decreasing the thickness of the n^- layers, t_{rr} can be made faster and V_F can be lowered. Based on these considerations, the density and diffusion depth of the p^+ layers, the lifetime killer diffusion density and the n^- layers were optimized, and as shown in Fig. 9, the SuperLLD3 series was commercialized with a higher density and shallower diffusion depth profile design than in Fuji's conventional LLD series.

5.　SuperLLD3 Series

Table 3 lists the absolute maximum ratings and electrical characteristics of the SuperLLD3. The rated current is from 8 to 20 A, and the package is either a TO-220AB, a TO-3P, a fully-insulated mold type TO-220F, or a surface mount type T-pack (S).

6.　Postscript

An overview of Fuji Electric's newly developed SuperLLD3 series has been presented above. This series has sufficient performance for application to current continuous mode power factor correction circuits, and is also effective in applications to the secondary rectification in a high-output power supply where high

Fig.9　Diffusion profile
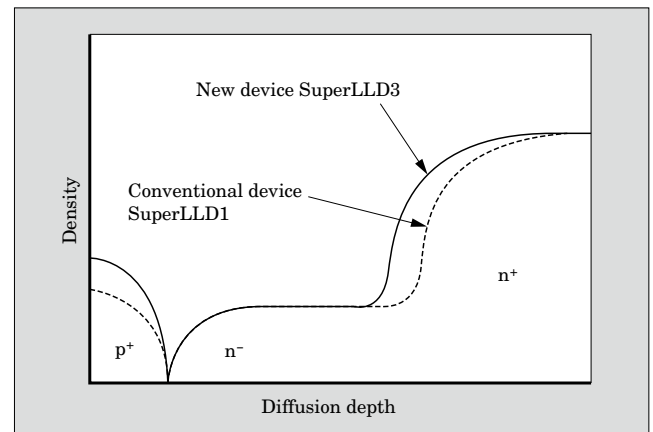
working voltage, high speed and low V_F characteristics are required. In the future, the power supply trends toward higher output and smaller size through harmonic current driving are expected to continue, and even lower power loss and lower noise emission will be required for the diodes used in such power supplies. Fuji Electric intends to continue to improve the characteristics and quality of high-speed diodes, including LLDs, SBDs and the like, and to expand its product lineup and provide even more effective products to the market.

References
(1) Onishi. Y. et al. Analysis on Device Structure for Next Generation IGBT. Proceedings of the 10th ISPSD. 1998. p.85-88.

SuperFAP-E³ Series of 6th Generation MOSFETs

Yukihito Hara
Tadanori Yamada
Yasushi Niimura

1. Introduction

With environmental problems drawing attention in recent years, electronic equipment and the switched mode power supplies (SMPS) installed in that equipment are being required to provide greater energy savings and resource conservation. The main challenges to realizing these objectives are achieving lower power consumption through increased efficiency, circuit simplification through a reduced number of components, and lower noise.

In consideration of the above, the power devices used in electronic equipment (including switched mode power supplies) are required to be low-loss, low-noise, damage resistant and easy to use. In particular, since EMI (electromagnetic interference) noise emissions must comply with various legal regulations, it may be obliged to change circuit constants or add filter circuits etc. in the final stage of electronic equipment design, and this may be time consuming for adjustments. Thus, to support the shorter design times of recent electronic equipment there is a growing need for low-noise devices for which EMI noise suppression is easy to implement.

Fuji Electric has a successful track record of combining low drain-source on-resistance and ultra high-speed switching to develop the SuperFAP-G series of low-loss power MOSFETs (metal-oxide-semiconductor field effect transistors) compatible with a drain-source voltage range of 100 to 900 V, and has contributed to realizing higher efficiency in electronic devices.

To satisfy market needs for low-loss, low-noise, damage resistant and easy-to-use power devices, Fuji Electric has recently developed the SuperFAP-E³ series of 6th generation MOSFETs that balance low-loss characteristics and low noise on high level and successfully combine high performance with ease of use. The characteristics of this new series are described below.

2. Product Overview

Table 1 compares the characteristics of the representative models of the newly developed SuperFAP-E³ series and conventional devices. The newly developed

Table 1 Comparison of SuperFAP-E³ series and conventional device characteristics (comparison for the same chip size)

Series	SuperFAP-E³ series	SuperFAP-G series (conventional series)
Model	FMA20N50E	2SK3683-01MR
Package	TO-220F	TO-220F
V_{DS}	500 V	500 V
I_D	±20 A	±19 A
P_D	95 W	95 W
$V_{GS (th)}$	3±0.5 V	4±1.0 V
$R_{DS (on) max}$	0.31 Ω	0.38 Ω

Fig.1 External appearance of SuperFAP-E³ series devices
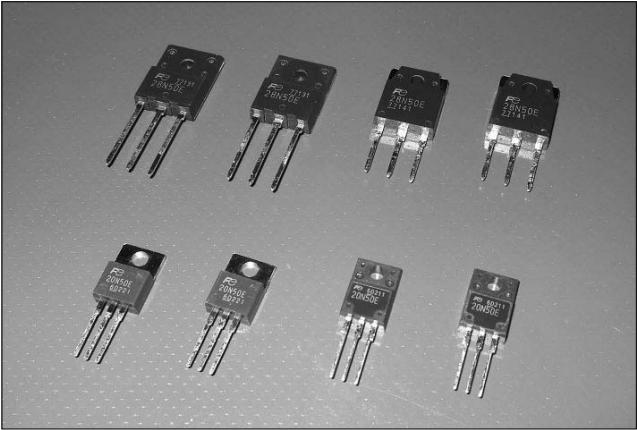
models realize an approximate 18% improvement in drain-source on-resistance compared to conventional devices of the same chip size, and also realize the industry's top-class of performance as planar type power MOSFETs. Figure 1 shows the external appearance of the SuperFAP-E³ series devices.

The SuperFAP-E³ series includes 500 V and 600 V (drain-source voltage) classes of devices, and the development of devices having a built-in zener diode between the gate and source, and devices having a higher speed parasitic diode are planned for the future. Table 2 lists representative characteristics of models ready for mass-production and model slated for a future product lineup.

Table 2 SuperFAP-E[3] series product list

Drain-source voltage BV_{DSS}	Drain current I_{D}	Drain-source on-resistance $R_{\mathrm{DS\,(on)}}$	Package					Remarks
			TO-220	TO-220F	T-pack (D2-pack)	TO-3P	TO-3PF	
500 V	16 A	0.380 Ω	FMP16N50E	FMA16N50E	FMB16N50E	—	—	In mass-production
	20 A	0.310 Ω	FMP20N50E	FMA20N50E	FMB20N50E	—	—	In mass-production
	7.5 A	0.790 Ω	FMP08N50E	FMA08N50E	FMB08N50E	—	—	In mass-production
	12 A	0.520 Ω	FMP12N50E	FMA12N50E	FMB12N50E	—	—	In mass-production
	23 A	0.245 Ω	—	FMA23N50E	—	FMH23N50E	FMR23N50E	In mass-production
	28 A	0.190 Ω	—	—	—	FMH28N50E	FMR28N50E	In mass-production
600 V	13 A	0.580 Ω	FMP13N60E	FMA13N60E	FMB13N60E	—	—	In mass-production
	16 A	0.470 Ω	FMP16N60E	FMA16N60E	FMB16N60E	—	—	In mass-production
	6 A	1.200 Ω	FMP06N60E	FMA06N60E	FMB06N60E	—	—	In mass-production
	10 A	0.790 Ω	FMP10N60E	FMA10N60E	FMB10N60E	—	—	In mass-production
	19 A	0.365 Ω	—	FMA19N60E	—	FMH19N60E	FMR19N60E	In mass-production
	23 A	0.280 Ω	—	—	—	FMH23N60E	FMR23N60E	In mass-production

3. Design Measures

Requested MOSFET characteristics are summarized in Table 3. Lower loss requires lower on-resistance and lower switching loss. Reducing the gate resistance to suppress the switching loss, however, results in an increase in emission noise. In other words, a tradeoff relation exists between switching loss and emission noise. Moreover, overshoot of the drain voltage is generated when the large current flowing at startup of the power supply is cutoff, and if this overshoot causes avalanche breakdown in the MOSFET, it is important that the MOSFET will not become damaged by the avalanche current. Furthermore, there are also requests for a MOSFET that is easy to use and whose operation is not easily affected by circuit board layouts that change according to the particular electronic equipment design.

3.1 Design of the cellular part

In the conventional SuperFAP-G series, as a result of arranging the p-wells densely and minimizing the spacing between the p-wells, a QPJ (quasi-plane junction) that is analogous to a planar pn junction was utilized. In order to lower the on-resistance even further, a lower resistance wafer must be used, but with the QPJ, sufficient resistance to avalanching could not be ensured when using a lower capability wafer. Thus, to improve the avalanche capability of the newly devel-

Table 3 Market needs of switched mode power supplies and requested characteristics of MOSFETs

Market needs of switched mode power supplies	Requested characteristics of MOSFETs
Low loss and low noise	○ Low on-resistance (combined with high avalanche capability) ○ Design that balances switching loss and emission noise (improved tradeoff)
Damage resistant	○ High avalanche resistance (combined with low on-resistance characteristics)
Easy to use	○ V_{GS} ringing not likely to occur even in the source common wiring is long

oped device series based on the conventional QPJ, the p-well width is made narrower, and locations of electric field concentrations are moved from the pn junction at a channel bottom to the bottom surface of a p-well so that the avalanche current flowing into a parasitic bipolar transistor is reduced, and the avalanche capability is aimed to improve. As a result, a wafer having lower resistance than in the SuperFAP-G series may be used while achieving lower on-resistance characteristics and the same high avalanche capability as with the conventional device series. Figure 2 shows the relation between drain-source on-resistance and drain-source breakdown voltage ($R_{\mathrm{DS(on)}} - BV_{\mathrm{DSS}}$). Figure 2 reveals that $R_{\mathrm{DS(on)}}$ has been improved by 18% compared to the conventional device series.

Emission noise is correlated to the switching dv/dt of the drain voltage. Namely, the tradeoff between

switching loss and switching dv/dt must be improved. These characteristics are determined by the ratio of the charge time constant to the gate-drain capacitance (C_{GD}) and the drain-source capacitance (C_{DS}). Figure 3 shows a cross-sectional drawing of the power MOSFET and its equivalent capacitance. C_{GD} is determined by the p-well spacing (gate electrode length) and C_{DS} is determined by the p-well width, and these had to be optimized in the design. In the conventional device series, as a result of the QPJ, low on-resistance characteristics, ultra high-speed switching characteristics and low gate charge (Q_G) characteristics were realized[1]. However, in order to improve the switching loss and switching dv/dt, C_{GD}/C_{DS} had to be made larger than in the conventional device series. But if the p-well spacing is enlarged, electric fields increase in the p-well corner areas, the QPJ state collapses, the break-

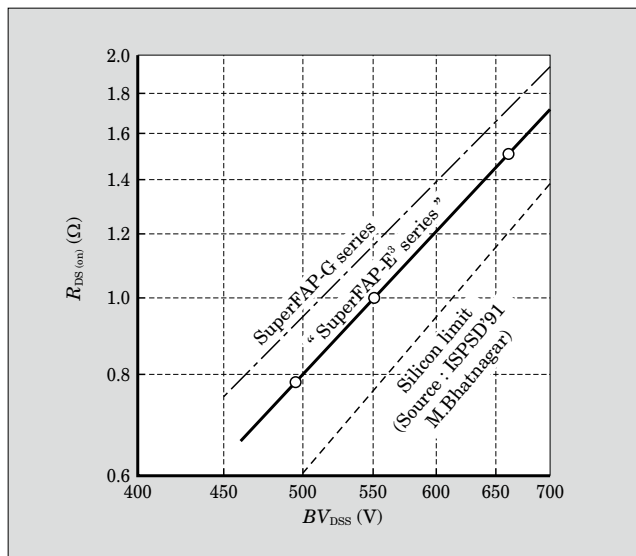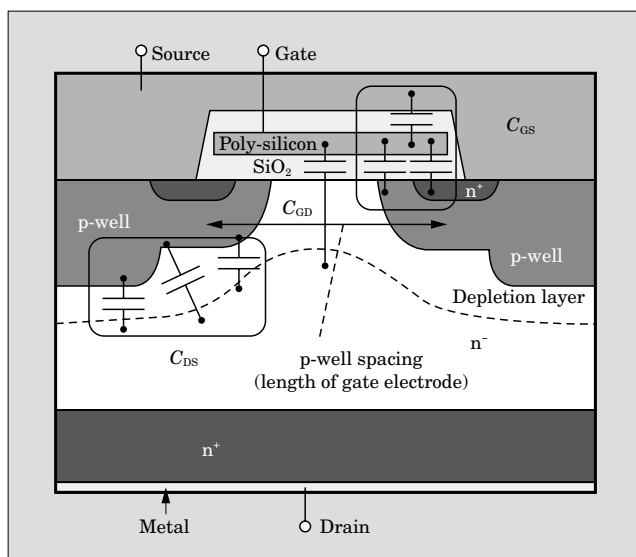Fig.2 $R_{DS(on)}$ – BV_{DSS} characteristics

Fig.3 Power MOSFET cross-sectional drawing and equivalent circuit

down voltage drops and on-resistance characteristics deteriorate. Moreover, higher electric fields in the corner areas lead to the problem of decreased avalanche capability. Thus, in order to maintain the QPJ while improving low on-resistance characteristics and the controllability of switching based on gate resistance, the concentration of the n-substrate in the area facing the gate electrode was optimized, and the p-well spacing was enlarged to mitigate the concentration of electric fields. This improved the ratio of C_{GD}/C_{DS} to approximately twice as big as that of the conventional device series.

3.2 Optimized guard-ring technology

With the conventional SuperFAP-G series, in order to mitigate the concentration of electric fields at withstand voltage structures resulting from the use of a low-resistance wafer, an optimized guard-ring structure having non-uniform pitch is used to support the generated withstand voltage close to the silicon limit at the cellular part. In contrast to a field plate structure, this optimized guard-ring is not susceptible to surface charge, and has high reliability, but also has the problem of a long edge length and a poor chip area utilization rate. In the SuperFAP-E[3] series, the guard-ring structure was optimized in order to improve the generated withstand voltage per unit length. Optimization of the guard-ring structure enabled the realization of an edge length of approximately 40% that of the conventional device series, while ensuring high reliability.

4. Effect of the SuperFAP-E[3] and Example Application to Power Supply

The SuperFAP-E[3] series has low loss and high avalanche capability, and an improved tradeoff between emission noise and switching loss. Comparisons between the conventional device series and the Super-FAP-E[3] series are described below.

Fig.4 Temperature rise in offline converter of switched mode power supply for LCD-TV
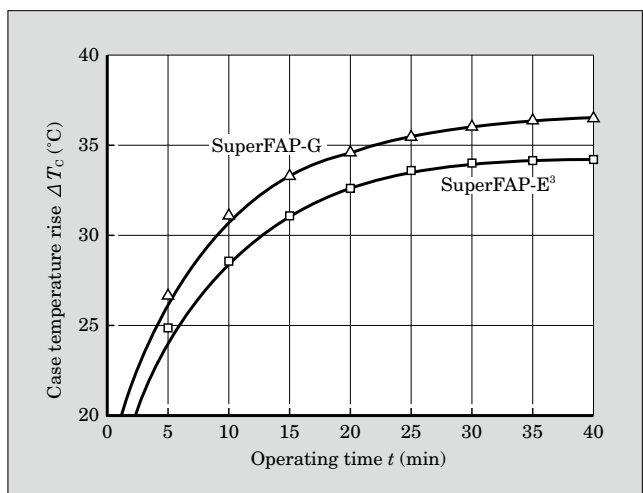
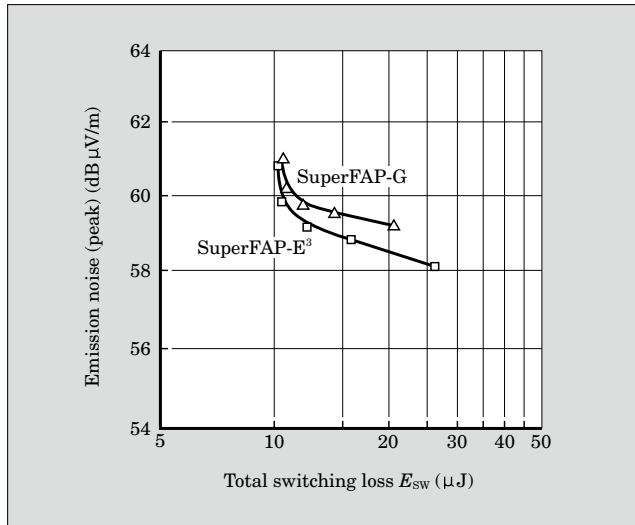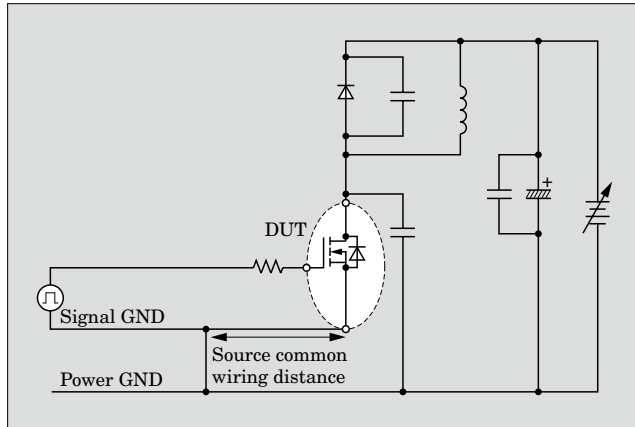Fig.5 Emission noise – switching loss characteristic
      (in open frame state)

Fig.6 Simulated circuit configuration

Fig.7 Source common wiring and ringing phenomenon in
      simulated circuit

(a) SuperFAP-E^3 series (common part wiring length : L = 30 mm)

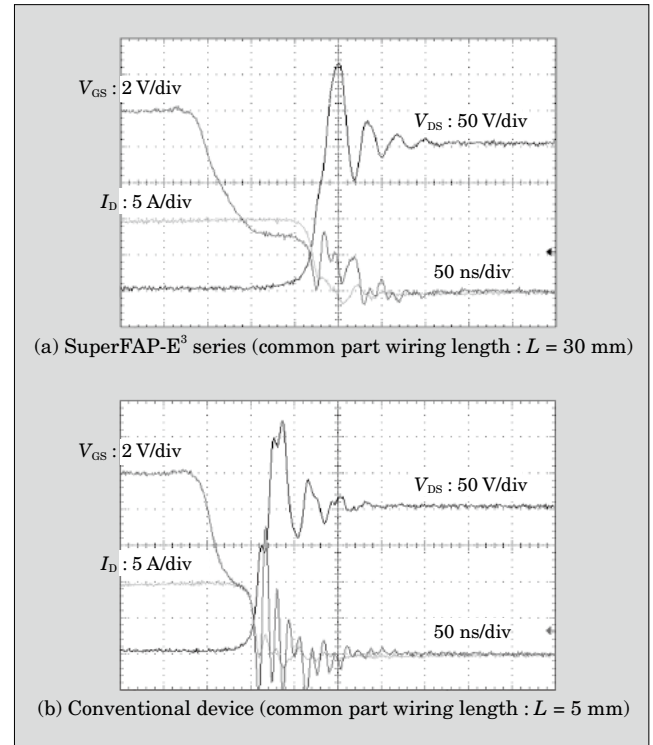(b) Conventional device (common part wiring length : L = 5 mm)

4.1 Temperature rise comparison

Figure 4 shows the relationship between conduction time and temperature rise of the device surface in the offline converter of switched mode power supply for LCD-TV. The gate resistance is adjusted to find the appropriate turn-on dv/dt of the drain voltage, which is the drive condition, and the surface temperature of the device is approximately 2 °C lower for the SuperFAP-E^3 series than in the case of the conventional device series.

4.2 Switching characteristics and emission noise verification

Figure 5 shows the relationship between switching loss and emission noise in a typical open frame power supply. Compared to the conventional device series, the SuperFAP-E^3 series has an improved tradeoff relation between switching loss and switching dv/dt of the drain voltage, and exhibits a large change in the level of emission noise in the actual range of gate resis-

tances used in an actual machine, thus improving the controllability of switching dv/dt of the drain voltage by gate resistance.

4.3 V_{GS} ringing comparison

Figure 6 shows the configuration of a simulated circuit and Fig. 7 shows the turn-off waveform of the simulated circuit. With the SuperFAP-E^3 series, even if the source common wiring distance is six times that of the conventional device series, the gate-source voltage (V_{GS}) ringing and waveform distortion will be at the same level or less.

From the above, it is clear that the SuperFAP-E^3 series provides more freedom for the circuit board layout, has a lower incidence rate of mis-operation, and is easier to use than the conventional device series.

5. Postscript

Characteristics of Fuji Electric's newly developed SuperFAP-E^3 series of low-loss and low-noise power MOSFETs have been described above. Fuji Electric intends to expand the product lines of 500 V and 600 V class devices using the newly developed cellular part and optimized guard-ring technology without delay.

Reference
(1) Kobayashi, T. et al. High-Voltage Power MOSFETs Reached Almost to the Silicon Limit. Proceedings of ISPSD'01, 2001, p.435-438.

FA5553/5547 Series of PWM Control Power Supply ICs with Multi-functionality and Low Standby Power

Masanari Fujii
Hiroshi Maruyama
Kokou Boku

1. Introduction

In recent years, global environmental warming has come to be addressed as a worldwide problem and energy savings has become critical for all electric products. In particular, televisions, audio components, notebook computers, printers and other such peripheral devices that are often continuously plugged into an electrical outlet remain in their standby state for a longer duration of time than their actual time of usage, and therefore functions for reducing the power consumption during standby have become essential. Requests for lower standby power consumption in power supply units have also intensified year after year.

In response to these requests, Fuji Electric has already developed a series of control ICs for use in switching mode power supply units to convert commercial AC power (100 V or 240 V) to a DC power supply. Recently, Fuji Electric has developed the FA5553/5547 series of 8-pin current mode PWM (pulse width modulation) control power supply ICs which feature enhanced low standby power performance and added protection functions suitable for various products. An overview of this new product series is presented below.

2. Product Overview

Fuji Electric has developed a series of AC-DC power supply ICs for driving externally attached power MOSFETs fabricated using a 30 V CMOS (complementary metal-oxide-semiconductor) process, and this newly developed IC series is listed in Table 1. This IC series is used as a PWM IC on the primary side in the conceptual diagram of a switching mode power supply shown in Fig. 1.

2.1 Characteristics

As indicated in Table 1 each unit type is provided

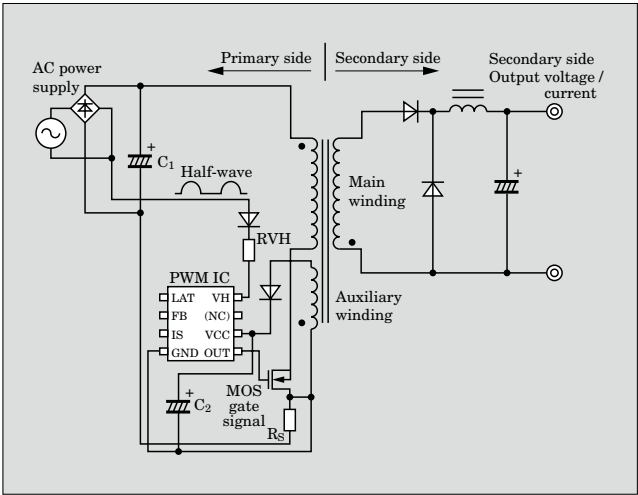Fig.1 Conceptual diagram of switching mode power supply

Table 1 Characteristics of PWM IC series for low standby power

Series	Model	Package	Power supply configuration	Input range	Operating frequency	Protection function				Low standby power function		
						Overload	Over-voltage	Latch by an external signal (overheat)	Brown-out	Startup circuit	Min. operating frequency during standby	Overload line compensation loss
FA5528	FA5528	SOP/DIP8	Flyback	10 to 26 V	60 kHz	Timer latch	Latch	Yes	No	Yes	1.1 kHz	< 70 mW
FA5553	FA5553	SOP/DIP8	Flyback	10 to 26 V	60 kHz	Auto-restart	Latch	Yes	No	Yes	0.35 kHz	< 5 mW
	FA5554					Timer latch						
	FA5566				100 kHz	Auto-restart						
	FA5567					Timer latch						
FA5547	FA5546	SOP/DIP8	Flyback	10 to 26 V	60 kHz	Auto-restart	Latch	Yes	Yes	Yes	0.5 kHz	< 5 mW
	FA5547					Timer latch						

☐ : New product

with a built-in 500 V high voltage startup circuit as in the conventional FA5528 series and is also provided with a function to reduce the operating frequency during standby according to the load. Compared to the conventional series, the minimum operating frequency has been reduced and the loss associated with compensating for the input voltage dependency of the overload detection level (i.e. overload line compensation loss) has also been reduced for the new product series to realize even lower levels of power consumption during standby operation. Meanwhile, in terms of protection functions, a low AC input voltage protection (brown-out) function has been added to the FA5547 series. This function shares the pins used by the above-described startup circuit so that, without increasing the number of pins, a package can be realized with the same number of pins as in the past.

The power supply protection functions and number of externally attached components are listed in Table 2. With the FA5553 series, an external latch type overheat protection function is configured by a thermistor only, enabling the number of external components to be reduced by two components compared to the conventional series. Moreover, with the FA5547 series, in addition to the abovementioned overheat protection, a current limiting function that operates in response to a pulsed load current and is required in power supply units having a load such as a motor, and a brown-out function are built into the IC, enabling the number of external components to be reduced by eight components compared to the conventional series and a reduction in cost of the power supply unit.

2.2 Low standby power consumption
(1) Startup circuit (common function)

Table 2 Power supply protection functions and number of externally attached components

(a) Power supplies that require overheat protection

| Model | Protection function | | | No. of external components |
	Overload	Over-voltage	Latch by an external signal (overheat)	
FA5528	Yes	Yes	Yes	17
FA5553 FA5554	Yes	Yes	Yes*	15

∗ Overheat detectoin possible with a thermistor only   ▭ : New product

(b) Power supplies having diverse protection functions

| Model | Protection function | | | | | No. of external components |
	Overload	Current limiting	Over-voltage	Latch by an external signal (overheat)	Brown-out	
FA5528	Yes	No	Yes	Yes	No	25
FA5546 FA5547	Yes	Yes	Yes	Yes*	Yes	17

∗ Overheat detectoin possible with a thermistor only   ▭ : New product

Figure 2 shows the method for connecting the VH pin to the half-wave rectified AC input voltage. When the power supply is turned on, the current supplied from the startup circuit to the VCC pin charges the capacitor C2 connected to the VCC pin, causing the VCC voltage to rise, the IC to be activated and the power supply to start operation. The current supplied from the VH pin to the VCC pin is largest in the state where the VCC pin voltage is 0 V, and the supplied current decreases when the VCC pin voltage increases. Moreover, a resistor is connected in series with the VH pin in order to prevent IC damage due to surge voltage on the AC line or elsewhere.

(2) Minimum operating frequency during standby (common function)

When the load is heavy, the switching frequency is fixed at the 60 kHz or 100 kHz operating frequency listed in Table 1. However, a function is provided for automatically decreasing the switching frequency when the load is light, such as during standby, so as to reduce loss. As shown in Fig. 3, when the load is light, the frequency decrease is proportional to the FB pin voltage and is nearly linear down to a minimum frequency f_{min} (0.35 kHz).

(3) Reduction of overload line compensation loss (common function)
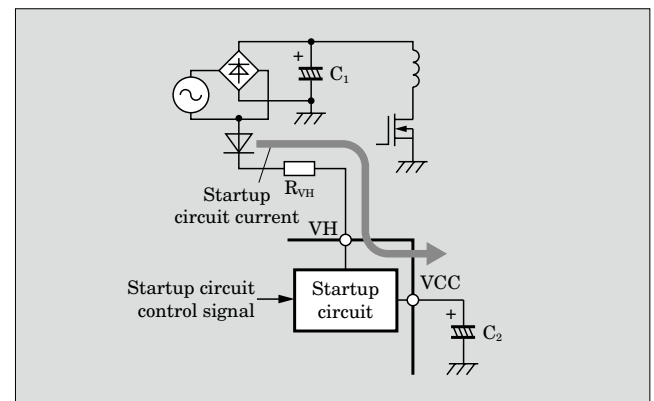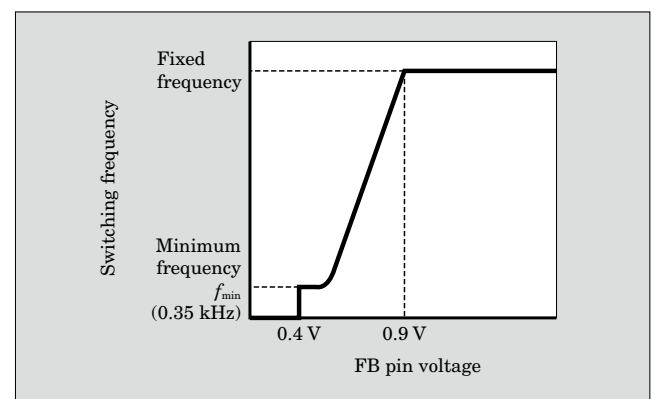
Fig.2 Startup circuit

Fig.3 Relationship between switching frequency and FB pin voltage

Since the gradient of the inductance current of a transformer differs according to the input voltage, the overcurrent values associated with an overload condition will be different. Previously, as shown in Fig. 4 (b), a resistor R_4 is connected between the current detection resistor R_s and the IS pin, and a resistor R_5 is connected between the AC line (after rectification and smoothing) and the IS pin, and since a high voltage is applied to resistor R_5, the loss of 70 mW at this portion was particularly large. Thus, with the new product series, the IS detection polarity was changed from plus detection to minus detection. As a result, as shown in Fig. 4 (a), a resistor R_9 is connected between the auxiliary winding and the IS pin, enabling a decrease in the input voltage dependency of the overload detection level and a loss at this portion of 5 mW which is 1/14th that of the conventional product series.

2.3 Protection functions

(1) External latch type overheat protection (common function)

By connecting a thermistor TH to the LAT pin as shown in Fig. 5, the IC will enter the latch mode for LAT pin voltages of 1.05 V or less.

The protection functions of the FA5547 series only

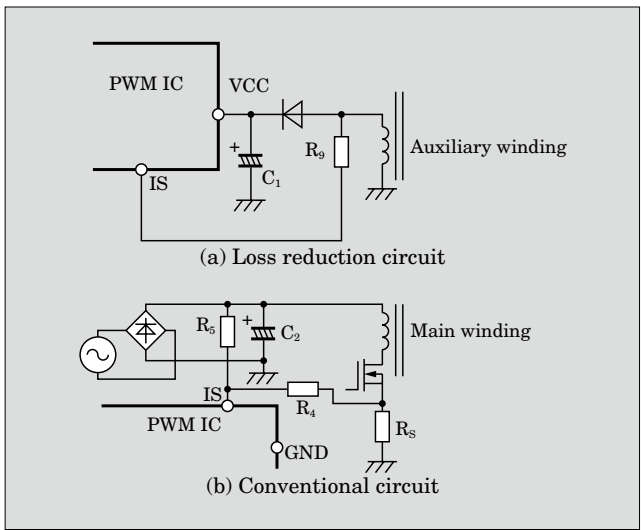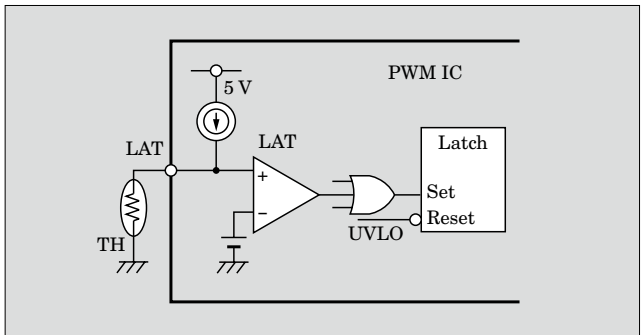Fig.4 Overload line compensation circuit

(a) Loss reduction circuit

(b) Conventional circuit

Fig.5 External latch type overheat protection circuit

are described below.

(2) Low AC input voltage protection (brown-out)

As shown in Fig. 6, the AC input voltage is monitored at the VH pin and is input, via a startup circuit, to a comparator. Figure 7 shows conceptual diagrams of the brown-out release (brown-in) and the brown-out detection operation when using the half-wave input of the AC input voltage at the VH pin. Figure 7 (a) shows the operation during brown-in, wherein when the half-wave rectified input becomes greater than the brown-in detection voltage threshold value, the IC begins its switching operation and the secondary-side output voltage rises. Figure 7 (b) shows the operation during brown-out, wherein the IC switching operation stops 50 ms after the half-wave rectified input becomes less than the comparator's brown-out detection voltage threshold value.

(3) Overload protection (current limiting)

Functions to protect against pulsed load current as
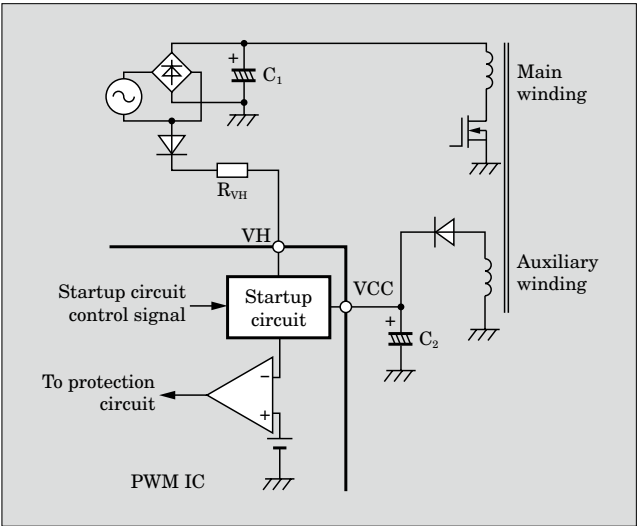
Fig.6 Brown-out detection circuit

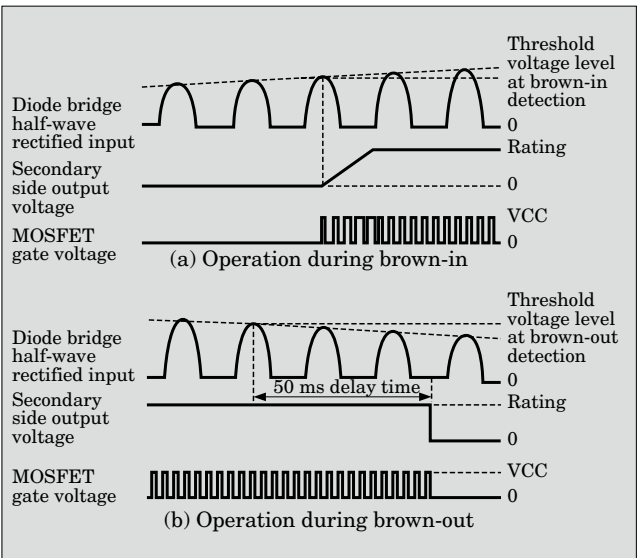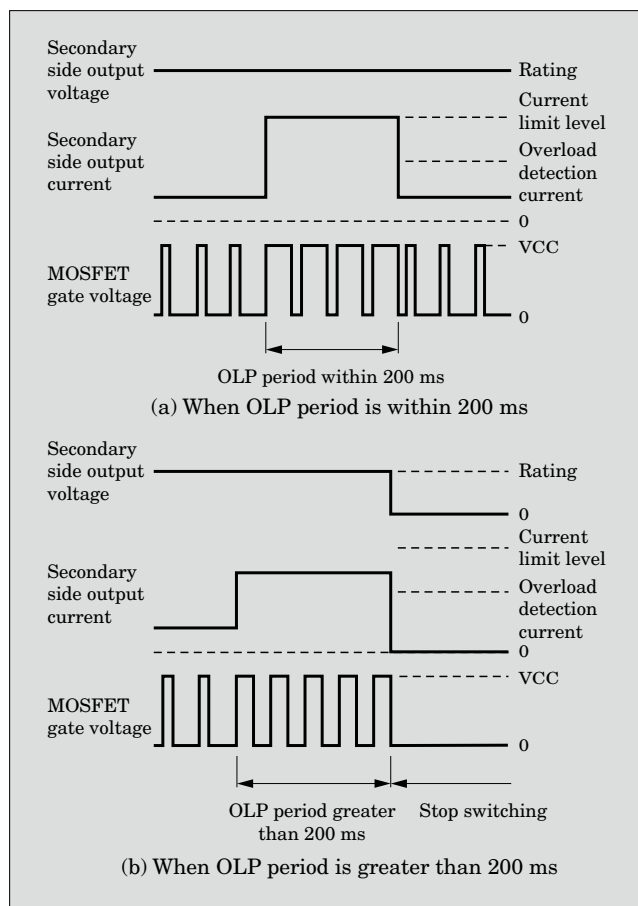Fig.7 Conceptual diagram of brown-in and brown-out

(a) Operation during brown-in

(b) Operation during brown-out

Fig.8 Conceptual diagram of overcurrent operation in re-
sponse to pulsed load current

(a) When OLP period is within 200 ms

(b) When OLP period is greater than 200 ms

Fig.9 Relationship between load current and power supply
efficiency

(1)   Input voltage: 90 to 264 V AC, 50/60 Hz
(2)   Output: 19 V DC, 0 to 3.42 A (65 W)
(3)   IC used: FA5553 (60 kHz operating frequency)

Figure 9 shows the relationship between load cur-
rent and power supply efficiency for input voltages
of 100 V and 264 V AC, and a load current of 1.5 A or
less. A high efficiency of at least 80% is reached when
the input voltage is 100 V AC and the load current is
80 mA or more and when the input voltage is 264 V AC
and the load current is 0.3 A or more. In particular,
there is only a small decrease in efficiency in regions
where the load current is low. Figure 10 shows the cir-
cuit diagram of this power supply.

3.2 Operating frequency characteristics

Figure 11 shows the relationship between load
current and operating frequency for input voltages of
100 V and 264 V AC. In the load current range from
0 to 0.9 A, the operating frequency decreases linearly,
and the IC's light load frequency decreasing function,
shown in Fig. 3, operates in this range. This function
enables a high power supply efficiency to be main-
tained even in the light load region with the power
supply efficiency shown in Fig. 9.

3.3 Standby power characteristics

Figure 12 shows the relationship between input
voltage and input power (standby power) during un-
loaded output operation. In the input voltage range
of 90 to 240 V AC, the input power is small as 0.1 W.
These characteristics are made possible by embedding
a startup circuit into the IC, decreasing the operating
frequency during light load operation, and decreasing
the overload line compensation loss.

As described above, use of the newly developed
FA5553 series and the FA5547 series enable higher ef-
ficiency due to lower standby power and various types
of required protection functions to be realized with a

well as overload protection are required in some power
supplies used for ink jet printers and other such motor
loads. Figure 8 shows conceptual diagrams of the over-
current operation in response to pulsed load current.
Figure 8 (a) shows the case in which when the overload
period is not more than 200 ms, even if the second-
ary-side output current is larger than the overload
detection current level, the IC will continue switching
and the secondary-side output voltage will be main-
tained until reaching the current limiting level. At
loads above the current limiting level, the primary-side
switching current is limited pulse-by-pulse, and the
secondary-side output voltage decreases. However, as
in Fig. 8 (b), if the load period is 200 ms or greater, the
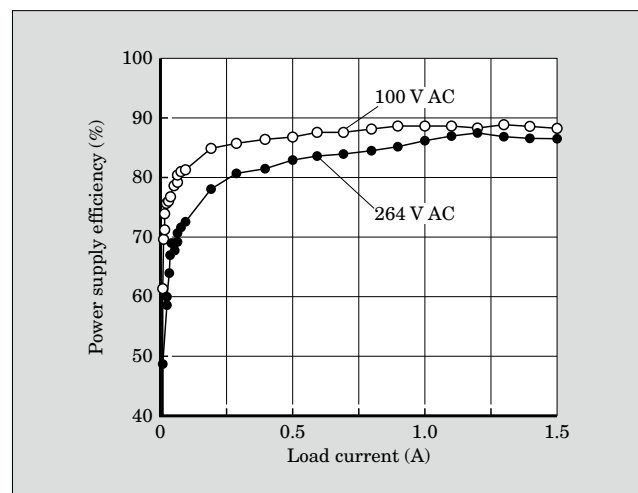IC is latched and stopped and the switching operation
is also stopped.

3.   Application to Power Supply Circuit

Characteristics of a switching mode power supply
that uses the FA5553 are described below.

3.1 Power supply efficiency characteristics

Main specifications of the power supply are listed
below.

Fig.10 Power supply circuit diagram
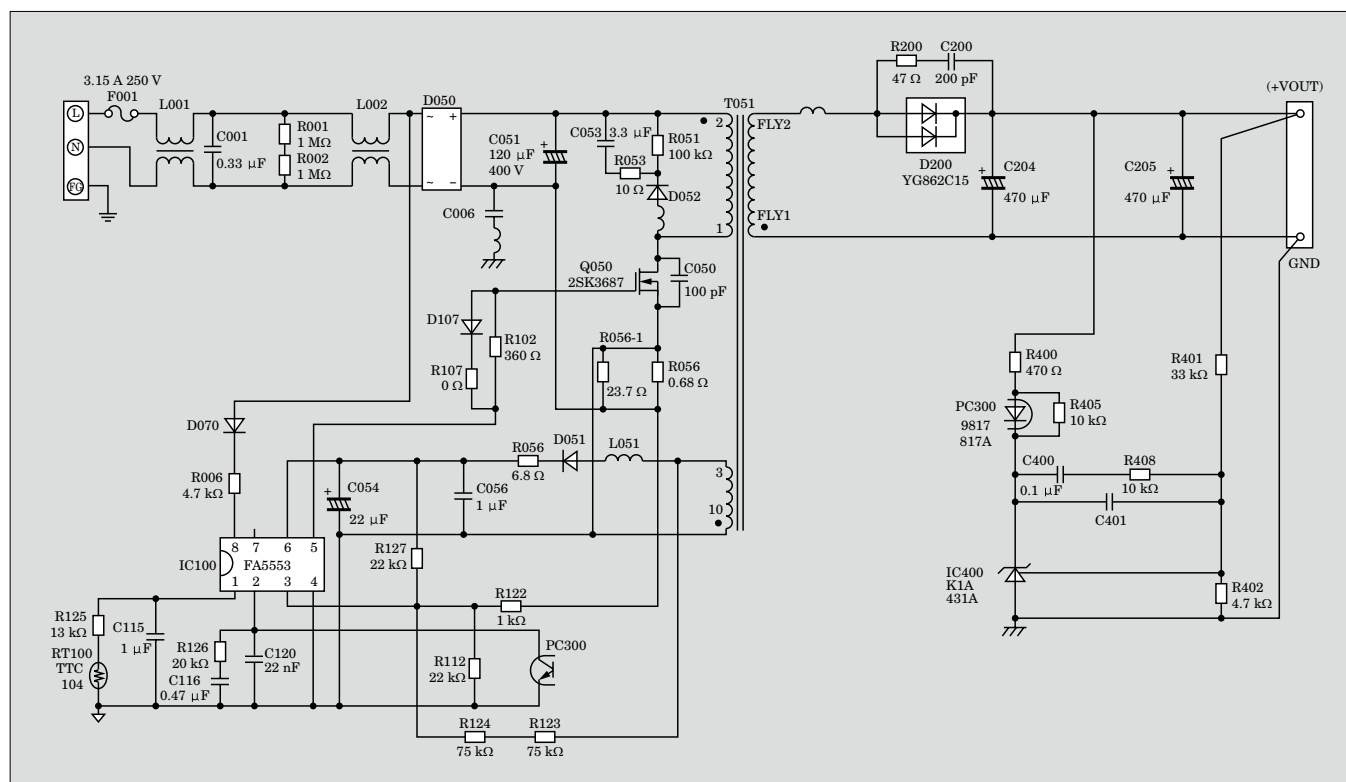
Fig.11 Relationship between load current and operating frequency

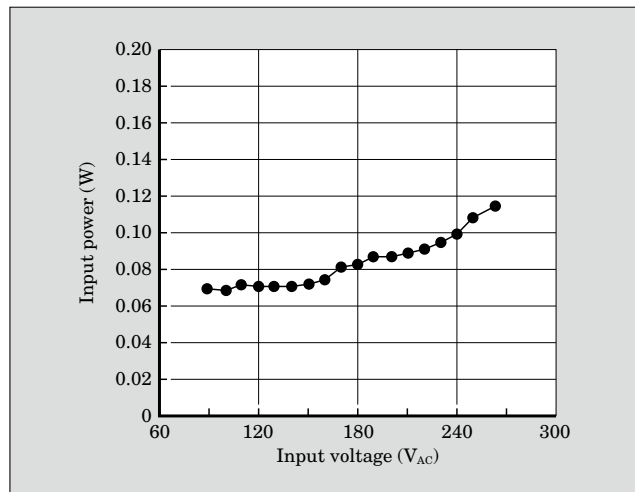Fig.12 Relationship between input voltage and input power for unloaded output
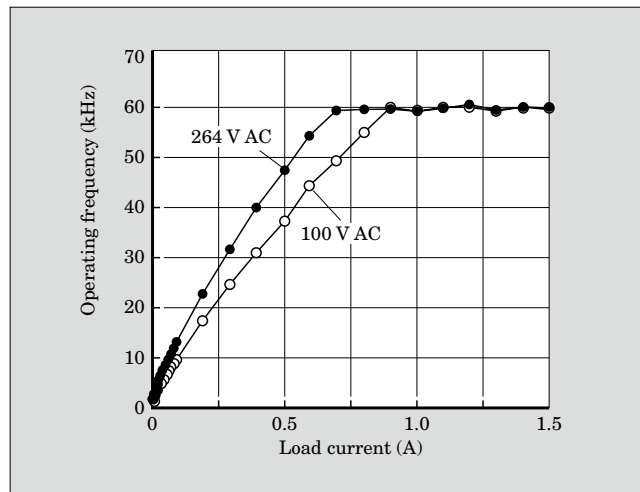
small number of components.

4. Postscript

A power supply IC that supports low standby power and that enables various required protection functions to be configured with a small number of components has been described. In this field, requests for lower power consumption are expected to intensify in the future, and Fuji Electric intends to continue to enhance functionality and reduce the number of components to develop easy-to-use products.

Global Network

AMERICA

● **FUJI ELECTRIC CORP. OF AMERICA**
USA
Phone: +1-201-712-0555   Fax: +1-201-368-8258

◆ **FUJI ELECTRIC DEVICE TECHNOLOGY AMERICA INC.**
USA
Phone: +1-732-560-9410   Fax: +1-732-457-0042

EU

■ **FUJI ELECTRIC HOLDINGS CO., LTD.**
Erlangen Representative Office
GERMANY
Phone: +49-9131-729613   Fax: +49-9131-28831

● **FUJI ELECTRIC FA EUROPE GmbH**
GERMANY
Phone: +49-69-6690290   Fax: +49-69-66902958

● **FUJI ELECTRIC DEVICE TECHNOLOGY EUROPE GmbH**
GERMANY
Phone: +49-69-6690290   Fax: +49-69-6661020

◆ **FUJI ELECTRIC FRANCE S.A.**
FRANCE
Phone: +33-4-73-98-26-98   Fax: +33-4-73-98-26-99

ASIA
East Asia

■ **FUJI ELECTRIC HOLDINGS CO., LTD.**
China Representative Office (Shanghai)
CHINA
Phone: +86-21-5496-3311   Fax : +86-21-5496-0189

■ **FUJI ELECTRIC HOLDINGS CO., LTD.**
China Representative Office (Beijing)
CHINA
Phone: +86-10-6505-1264   Fax: +86-10-6505-1851

● **FUJI ELECTRIC FA (SHANGHAI) CO., LTD.**
CHINA
Phone: +86-21-5496-1177   Fax: +86-21-6422-4650

◆ **FUJI ELECTRIC (CHANGSHU) CO., LTD.**
CHINA
Phone: +86-512-5284-5642   Fax: +86-512-5284-5640

◆ **WUXI FUJI ELECTRIC FA CO., LTD.**
CHINA
Phone: +86-510-8815-2088   Fax: +86-510-8815-9159

◆ **FUJI ELECTRIC DALIAN CO., LTD.**
CHINA
Phone: +86-411-8762-2000   Fax: +86-411-8762-2030

◆ **FUJI ELECTRIC MOTOR (DALIAN) CO., LTD.**
CHINA
Phone: +86-411-8763-6555   Fax: +86-411-8762-4077

● **FUJI ELECTRIC MOTOR (SHANGHAI) CO., LTD.**
CHINA
Phone: +86-21-5239-9681   Fax: +86-21-5239-9680

◆ **SHANGHAI FUJI ELECTRIC SWITCHGEAR CO., LTD.**
CHINA
Phone: +86-21-5718-1495   Fax: +86-21-5718-5745

◆ **SHANGHAI FUJI ELECTRIC TRANSFORMER CO., LTD.**
CHINA
Phone: +86-21-5718-1495   Fax: +86-21-5718-5745

■:Representative Office ●:Sales Base ◆:Manufacturing Base

◆ **FUJI ELECTRIC SYSTEMS(SHANGHAI) CO., LTD.**
CHINA
Phone: +86-21-5496-2211   Fax: +86-21-6417-6672

◆ **DALIAN FUJI BINGSHAN VENDING MACHINE CO., LTD.**
CHINA
Phone: +86-411-8730-5902   Fax: +86-411-8730-5911

● **DALIAN JIALE VENDING MACHINE OPERATION CO., LTD.**
CHINA
Phone: +86-411-8665-0277   Fax: +86-411-8596-2732

◆ **HANGZHOU FUJI REFRIGERATING MACHINE CO., LTD.**
CHINA
Phone: +86-571-8621-1661   Fax: +86-571-8821-0220

◆ **FUJI ELECTRIC (SHENZHEN) CO., LTD.**
CHINA
Phone: +86-755-2734-2910   Fax: +86-755-2734-2912

● **FUJI ELECTRIC FA (ASIA) CO., LTD.**
HONG KONG
Phone: +852-2311-8282   Fax: +852-2312-0566

● **FUJI ELECTRIC DEVICE TECHNOLOGY HONG KONG CO., LTD.**
HONG KONG
Phone: +852-2664-8699   Fax: +852-2664-8040

■ **FUJI ELECTRIC SYSTEMS CO., LTD.**
Taipei Representative Office
TAIWAN
Phone: +886-2-2501-1256   Fax: +886-2-2501-1250

● **FUJI ELECTRIC TAIWAN CO., LTD.**
TAIWAN
Phone: +886-2-2515-1850   Fax: +886-2-2515-1860

● **FUJI ELECTRIC FA TAIWAN CO., LTD.**
TAIWAN
Phone: +886-2-2370-2390   Fax: +886-2-2370-2389

◆ **ATAI FUJI ELECTRIC CO., LTD.**
TAIWAN
Phone: +886-3-321-3030   Fax: +886-3-321-7890

● **FUJI ELECTRIC FA KOREA CO., LTD.**
KOREA
Phone: +82-2-780-5011   Fax: +82-2-783-1707

Southeast Asia

■ **FUJI ELECTRIC SYSTEMS CO., LTD.**
Bangkok Representative Office
THAILAND
Phone: +66-2-308-2240   Fax: +66-2-308-2242

■ **FUJI ELECTRIC SYSTEMS CO., LTD.**
Jakarta Representative Office
INDONESIA
Phone: +62-21-572-4281   Fax: +62-21-572-4283

◆ **FUJI ELECTRIC (MALAYSIA) SDN. BHD.**
MALAYSIA
Phone: +60-4-403-1111   Fax: +60-4-403-1496

◆ **FUJI ELECTRIC PHILIPPINES, INC.**
PHILIPPINES
Phone: +632-844-6183   Fax: +632-844-6196

● **FUJI ELECTRIC SINGAPORE PRIVATE LTD.**
SINGAPORE
Phone: +65-6535-8998   Fax: +65-6532-6866

● **FUJI ELECTRIC FA SINGAPORE PRIVATE LTD.**
SINGAPORE
Phone: +65-6533-0010   Fax: +65-6533-0021

Fe

e-Front runners